

MONITORING LAND SUBSIDENCE OF AIRPORT USING INSAR TIME-SERIES  
TECHNIQUES WITH ATMOSPHERIC AND ORBITAL ERROR CORRECTIONS

ANIS AFIRAH BINTI MOHAMAD RADHI

UNIVERSITI TEKNOLOGI MALAYSIA

MONITORING LAND SUBSIDENCE OF AIRPORT USING INSAR TIME-  
SERIES TECHNIQUES WITH ATMOSPHERIC AND ORBITAL ERROR  
CORRECTIONS

ANIS AFIRAH BINTI MOHAMAD RADHI

A thesis submitted in fulfillment of the  
requirements for the award of the degree of  
Master of Science (Remote Sensing)

Faculty of Geoinformation and Real Estate  
Universiti Teknologi Malaysia

FEBRUARY 2017

*A special mention to my beloved parent....*

**Hj Mohamad Radhi bin Hj Othman,  
Hjh Nooraini binti Hj Yaacob ,**

*For giving me a lot of encouragement and strength to success.... love u both lillahi..*

*To my siblings,*

**Baish, Na, Iejad, Kak Min, and Qimi**

*Thanks for a lot of help in moral and financial support and understanding my  
situation*

*To friends,*

**“Geng aras 5”, “Geng usrah”, “Geng Master”**

*Thanks for all your support, advice and willing to be companions in good and bad  
times...*

*To all,*

*I hope we will meet again later in future and Jannah Insya Allah*

## ACKNOWLEDGMENT

*With The Name of Almighty Allah, Most Merciful Generous*

Thank god, for His mercy and kindness, this master degree finally completed. Infinite appreciation and gratitude to supervisor Dr Md Latifur Rahman Sarker for sharing ideas, provide encouragement and guidance to complete this master thesis. I also would like to thank the Ministry of Higher Education (MOHE) for providing grant (R.J130000.7827.4F689) entitled “Determination of Floodplain Change and its Impact on Flood Modelling Using Multi-Temporal DEM and Land Use/Land Cover from InSAR/SAR Technique” for financial support. Special thanks also goes to Japan Aerospace Exploration Agency (JAXA) for providing the ALOS data, under the project No. P1387002.

Sincere appreciation also goes out to all the lecturers and staff of the Department of Geomatics for their cooperation, guidance and assistance provided during my master study at UTM. Thank you also specially goes to lab mates and floor mates which together in this struggle and also the unwavering support and invaluable experience that we have over 3 years of our journey.

Lastly I would like to thank everyone who helped directly or indirectly in completing this project. Without you guys it means nothing to me. And my guideline, the very inspiration words (2:11, 12,164; 4:78-79; 23:17-22). Thank you so much.

## ABSTRACT

Land subsidence is one of the common geological hazards worldwide and mostly caused by human activities including the construction of massive infrastructures. Large infrastructure such as airport is susceptible to land subsidence due to several factors. Therefore, monitoring of the land subsidence at airport is crucial in order to prevent undesirable loss of property and life. Remote sensing technique, especially Interferometric Synthetic Aperture Radar (InSAR) has been successfully applied to measure the surface deformation over the past few decades although atmospheric artefact and orbital errors are still a concerning issue in this measurement technique. Multi-temporal InSAR, an extension of InSAR technique, uses large sets of SAR scenes to investigate the temporal evolution of surface deformation and mitigate errors found in a single interferogram. This study investigates the long-term land subsidence of the Kuala Lumpur International Airport (KLIA), Malaysia and Singapore Changi Airport (SCA), Singapore by using two multi-temporal InSAR techniques like Small Baseline Subset (SBAS) and Multiscale InSAR Time Series (MInTS). General InSAR processing was conducted to generate interferogram using ALOS PALSAR data from 2007 until 2011. Atmospheric and orbital corrections were carried out for all interferograms using weather model, namely European Centre for Medium Range Weather Forecasting (ECMWF) and Network De-Ramping technique respectively before estimating the time series land subsidence. The results show variation of subsidence with respect to corrections (atmospheric and orbital) as well as difference between multi-temporal InSAR techniques (SBAS and MInTS) used. After applying both corrections, a subsidence ranging from 2 to 17 mm/yr was found at all the selected areas at the KLIA. Meanwhile, for SCA, a subsidence of about less than 10 mm/yr was found. Furthermore, a comparison between two techniques (SBAS and MInTS) show a difference rate of subsidence of about less than 1 mm/yr for both study area. SBAS technique shows more linear result as compared to the MInTS technique which shows slightly scattering pattern but both techniques show a similar trend of surface deformation in both study sites. No drastic deformation was observed in these two study sites and slight deformation was detected which about less than 20mm/yr for both study areas probably occurred due to several reasons including conversion of the land use from agricultural land, land reclamation process and also poor construction. This study proved that InSAR time series surface deformation measurement techniques are useful as well as capable to monitor deformation of large infrastructure such as airport and as an alternative to costly conventional ground measurement for infrastructure monitoring.

## ABSTRAK

Pemendapan tanah merupakan salah satu bencana geologi yang sering terjadi di seluruh dunia dan kebanyakannya disebabkan oleh aktiviti manusia termasuk pembinaan infrastruktur secara besar-besaran. Infrastruktur yang besar seperti lapangan terbang juga terdedah kepada masalah pemendapan tanah disebabkan oleh beberapa faktor. Oleh itu, pemantauan tanah mendap di lapangan terbang adalah penting untuk mengelakkan kerugian yang tidak diingini sama ada harta mahupun nyawa. Teknik penderiaan jauh, terutamanya radar apertur sintetik interferometer (InSAR) telah berjaya digunakan untuk mengukur perubahan bentuk muka bumi sejak beberapa dekad yang lalu walaupun artifak atmosfera dan ralat pada orbit masih menjadi isu dalam teknik pengukuran ini. Teknik multi temporal InSAR, iaitu lanjutan daripada InSAR, menggunakan set data pemandangan SAR yang besar untuk mengkaji evolusi temporal perubahan bentuk muka bumi dan mengurangkan ralat yang ditemui dalam satu interferogram tunggal. Kajian ini mengkaji pemendapan tanah untuk jangka masa yang panjang terhadap Lapangan Terbang Antarabangsa Kuala Lumpur (KLIA), Malaysia dan Lapangan Terbang Changi (SCA), Singapura dengan menggunakan dua teknik multi temporal InSAR iaitu garis asas bersubset kecil (SBAS) dan pengukuran siri masa InSAR pelbagai skala (MInTS). Proses asas InSAR dilakukan untuk menghasilkan interferogram dengan menggunakan data ALOS PALSAR dari 2007 hingga 2011. Pembedahan atmosfera dan orbit telah dijalankan ke atas semua interferogram menggunakan model cuaca iaitu julat pengantar ramalan cuaca pusat Eropah (ECMWF) dan teknik Peningkatan Secara Rangkaian sebelum membuat anggaran siri masa pemendapan tanah. Keputusan menunjukkan terdapat variasi pemendapan tanah selepas pembedahan (atmosfera dan orbit) serta perbezaan antara teknik-teknik InSAR (SBAS dan MInTS) yang digunakan. Selepas kedua-dua pembedahan dilakukan, pemendapan tanah antara 2 hingga 17 mm/tahun ditemui di semua kawasan yang terpilih di KLIA. Sementara itu, bagi SCA, pemendapan tanah kurang daripada 10 mm/tahun ditemui. Tambahan pula, perbandingan di antara kedua-dua teknik (SBAS dan MInTS) menunjukkan kadar perbezaan pemendapan tanah sebanyak kurang daripada 1 mm/tahun bagi kedua-dua kawasan kajian. Teknik SBAS menunjukkan hasil yang lebih linear berbanding dengan teknik MInTS yang menunjukkan sedikit corak serakan tetapi kedua-dua teknik menunjukkan arah aliran deformasi yang sama di kedua-dua kawasan kajian. Tiada deformasi permukaan yang ketara diperhatikan di kedua-dua tapak kajian dan sedikit deformasi permukaan dikesan iaitu kurang dari 20mm/tahun di kedua-dua kawasan kajian mungkin berlaku disebabkan oleh beberapa sebab termasuk penukaran guna tanah daripada tanah pertanian, proses penambakan tanah dan juga pembinaan yang tidak kukuh. Kajian ini membuktikan bahawa pengukuran siri masa deformasi permukaan menggunakan InSAR sangat berguna serta mampu untuk memantau deformasi di infrastruktur yang besar seperti lapangan terbang dan boleh digunakan sebagai alternatif kepada pengukuran konvensional di permukaan tanah yang mahal dalam pemantauan infrastruktur.

## TABLE OF CONTENTS

| CHAPTER  | TITLE                         | PAGE |
|----------|-------------------------------|------|
|          | <b>AUTHOR'S DECLARATION</b>   | ii   |
|          | <b>DEDICATION</b>             | iii  |
|          | <b>ACKNOWLEDGEMENT</b>        | iv   |
|          | <b>ABSTRACT</b>               | v    |
|          | <b>ABSTRAK</b>                | vi   |
|          | <b>TABLE OF CONTENTS</b>      | vii  |
|          | <b>LIST OF TABLES</b>         | xiii |
|          | <b>LIST OF FIGURES</b>        | xiv  |
|          | <b>LIST OF SYMBOLS</b>        | xix  |
|          | <b>LIST OF ABBREVIATIONS</b>  | xxii |
|          | <b>LIST OF APPENDICES</b>     | xxv  |
| <b>1</b> | <b>INTRODUCTION</b>           | 1    |
|          | 1.1 Background of Study       | 1    |
|          | 1.2 Problem statements        | 6    |
|          | 1.3 Research Objectives       | 9    |
|          | 1.4 Scope of the Study        | 11   |
|          | 1.5 Study Area                | 13   |
|          | 1.6 Significance of the Study | 15   |
|          | 1.7 Thesis Outline            | 17   |

|          |   |           |
|----------|---|-----------|
| <b>2</b> | <b>LITERATURE REVIEW</b>                                      | <b>18</b> |
| 2.1      | Radar   | 18        |
| 2.2      | Synthetic Aperture Radar (SAR)                                | 19        |
| 2.2.1    | Resolution  | 20        |
| 2.2.2    | SAR Geometrical Effects                                       | 21        |
| 2.2.3    | Satellite Orbit Configuration                                 | 22        |
| 2.2.4    | SAR Image   | 23        |
| 2.2.4.1  | SAR Amplitude Image   | 24        |
| 2.2.4.2  | SAR Phase Image   | 24        |
| 2.2.4.3  | Speckle   | 25        |
| 2.3      | Interferometry Synthetic Aperture Radar (InSAR)               | 26        |
| 2.3.1    | Interferometry Equations                                      | 27        |
| 2.3.2    | Altitude Ambiguity  | 30        |
| 2.3.3    | Orbit Ramp  | 30        |
| 2.3.4    | Atmospheric Phase Screen                                      | 31        |
| 2.3.5    | Deformation Phase   | 32        |
| 2.4      | InSAR Processing  | 32        |
| 2.4.1    | Interferogram Generation                                      | 33        |
| 2.4.2    | Interferometric Correlation (Coherence)                       | 35        |
| 2.4.3    | Filtering   | 37        |
| 2.4.4    | Phase Unwrapping  | 38        |
| 2.5      | Differential Interferometry Synthetic Aperture Radar (DInSAR) | 39        |
| 2.6      | Multi-Temporal Technique                                      | 41        |
| 2.6.1    | Small Baseline Subset (SBAS)                                  | 42        |
| 2.6.2    | Multiscale InSAR Time Series (MInTS)                          | 45        |
| 2.7      | Natural Characteristic of the Interferogram                   | 46        |
| 2.7.1    | Atmospheric Delay: Tropospheric Delay                         | 47        |
| 2.7.2    | Orbital Error   | 49        |
| 2.8      | Land Subsidence   | 52        |
| 2.9      | Land Subsidence Monitoring                                    | 54        |
| 2.10     | Land Subsidence Monitoring At Airport                         | 57        |
| 2.11     | Summary   | 59        |

|          |  |           |
|----------|--|-----------|
| <b>3</b> | <b>METHODOLOGY</b>                                       | <b>60</b> |
| 3.1      | Datasets   | 60        |
| 3.1.1    | ALOS PALSAR Sensor Data                                  | 60        |
| 3.1.2    | Data Selection And Data Availability                     | 62        |
| 3.1.2.1  | Data Availability for Kuala Lumpur International Airport | 63        |
| 3.1.2.2  | Data Availability at Singapore Changi Airport            | 64        |
| 3.1.3    | Software Description                                     | 65        |
| 3.2      | Processing Steps   | 66        |
| 3.3      | Generation of Differential Interferogram                 | 67        |
| 3.3.1    | Focusing   | 67        |
| 3.3.2    | Coregistration   | 68        |
| 3.3.3    | Interferogram Generation                                 | 70        |
| 3.3.4    | Removing Topography                                      | 72        |
| 3.3.5    | Coherence Generation                                     | 74        |
| 3.3.6    | Filtering  | 75        |
| 3.3.7    | Phase Unwrapping   | 77        |
| 3.3.8    | Geocoding  | 79        |
| 3.4      | Time-Series Analysis                                     | 81        |
| 3.4.1    | Stack preparation and Stack Preprocessing                | 81        |
| 3.4.2    | Atmospheric Correction                                   | 82        |
| 3.4.3    | Orbital Correction With Network De-Ramping               | 84        |
| 3.4.4    | Small Baseline Subset (SBAS)                             | 86        |
| 3.4.5    | Multiscale InSAR Time-Series                             | 88        |
| 3.4.5.1  | Interferogram Wavelet Transformation                     | 88        |
| 3.4.5.2  | Parametrization of The Wavelet Coefficients              | 89        |
| 3.4.5.3  | Inverse Wavelet Transformation                           | 91        |
| 3.5      | Land Subsidence Measurement                              | 92        |
| 3.6      | Summary  | 92        |

|          |   |           |
|----------|---|-----------|
| <b>4</b> | <b>RESULT AND ANALYSIS</b>  | <b>93</b> |
|          | 4.1 DInSAR Results  | 93        |
|          | 4.1.1 Raw data  | 93        |
|          | 4.1.2 Data focusing   | 95        |
|          | 4.1.3 Resample Image and Interferogram<br>building  | 98        |
|          | 4.1.4 Removing topography   | 100       |
|          | 4.1.5 Coherence computing   | 102       |
|          | 4.1.6 Filtering   | 105       |
|          | 4.1.7 Phase unwrapped and Geocode   | 107       |
|          | 4.2 Atmospheric Correction  | 117       |
|          | 4.2.1 Atmospheric Model: ECMWF  | 117       |
|          | 4.2.2 Atmospheric Correction Results<br>for KLIA  | 121       |
|          | 4.2.3 Atmospheric Correction Results<br>for SCA   | 123       |
|          | 4.3 Orbital Ramp Correction   | 125       |
|          | 4.3.1 Orbital Ramp Correction for KLIA  | 125       |
|          | 4.3.2 Orbital Ramp Correction for SCA   | 128       |
|          | 4.4 Land Deformation Measurement using SBAS   | 130       |
|          | 4.4.1 Land Deformation Measurement<br>using SBAS at KLIA  | 130       |
|          | 4.4.1.1 Without<br>Atmospheric and<br>Orbital correction  | 131       |
|          | 4.4.1.2 With atmospheric<br>and orbital<br>correction   | 133       |
|          | 4.4.1.3 Variation of Land<br>Deformation<br>Estimation before<br>and after the<br>atmospheric and<br>orbital correction | 135       |

|          |   |            |
|----------|---|------------|
| 4.4.2    | Land Deformation Measurement<br>using SBAS at SCA   | 141        |
| 4.4.2.1  | Without atmospheric<br>and orbital<br>correction  | 141        |
| 4.4.2.2  | With atmospheric<br>and orbital<br>correction   | 143        |
| 4.4.2.3  | Variation of Land<br>Deformation<br>Estimation before<br>and after the<br>atmospheric and<br>orbital correction | 146        |
| 4.5      | Land Deformation Measurement using MInTS  | 150        |
| 4.5.1    | Estimation of Land Deformation<br>using MInTS at KLIA   | 150        |
| 4.5.2    | Estimation of Land Deformation<br>using MInTS at SCA  | 152        |
| 4.5.3    | Comparison of deformation<br>Estimation between SBAS<br>and MInTS Techniques                                    | 154        |
| 4.5.3.1  | Comparison for KLIA   | 154        |
| 4.5.3.2  | Comparison for SCA  | 160        |
| 4.6      | Summary   | 164        |
| <b>5</b> | <b>DISCUSSION</b>   | <b>165</b> |
| <b>6</b> | <b>CONCLUSION AND RECOMMENDATION</b>  | <b>172</b> |
| 6.1      | Conclusion  | 172        |
| 6.2      | Recommendation  | 174        |

**REFERENCES**

**175**

Appendices A – H

**203-211**

**LIST OF TABLES**

| <b>TABLE NO</b> | <b>TILTLE</b>   | <b>PAGE</b> |
|-----------------|---|-------------|
| 3.1             | Data Configurations with Sensor Properties<br>(Source: ASF, 2016) | 61          |
| 3.2             | Specification of ALOS PALSAR data used for KLIA                   | 63          |
| 3.3             | Specification of ALOS PALSAR data used for SCA                    | 64          |

## LIST OF FIGURES

| FIGURE NO | TILTLE  | PAGE |
|-----------|---|------|
| 1.1       | Map of Langat Basin (Source: Bringemeier, 2001)   | 14   |
| 1.2       | Singapore Changi Airport (red circle) which<br>built on reclaimed land (Source: UTexas, 2016) | 15   |
| 2.1       | Azimuth resolutions in top view (Source: Unavco, 2008)  | 20   |
| 2.2       | Range resolution from end view (Source: Unavco, 2008)   | 21   |
| 2.3       | Radar foreshortening, layover, and shadow effects<br>(Source: Hensley <i>et al.</i> , 2007)   | 22   |
| 2.4       | Concept of ascending and descending orbits<br>(Source: Parviz, 2012)                          | 23   |
| 2.5       | Emitted and backscattered sinusoidal signal<br>(Source: Goudarzi, 2010)                       | 25   |
| 2.6       | Example of speckle noise (Source: Parbleu, 2007)  | 26   |
| 2.7       | InSAR geometry (Source: Luzi, 2010)   | 29   |
| 2.8       | Basic DInSAR processing steps (Source: Hu <i>et al.</i> , 2014)                               | 33   |
| 2.9       | Steps for MInTS (Source: Lin <i>et al.</i> , 2010)  | 46   |
| 3.1       | AUIG2 provided by JAXA  | 62   |
| 3.2       | Overall methodology   | 66   |
| 3.3       | SLC image which contain amplitude (left) and phase<br>(right)                                 | 68   |
| 3.4       | Example of coregistration (Source: Zou <i>et al.</i> , 2009)                                  | 70   |

|      |  |     |
|------|--|-----|
| 3.5  | Generated interferogram by using complex conjugate multiplication for KLIA study area                              | 72  |
| 3.6  | DEM for KLIA (left) and SCA (right) study area   | 73  |
| 3.7  | Correlation of the phase of interferogram pair 20070210-20070628   | 75  |
| 3.8  | Comparison between flattened interferogram (left) and filtered interferogram (right) by using the Goldstein filter | 77  |
| 3.9  | Unwrapped interferogram using SNAPHU algorithm for interferogram pair 20070210-20070628 at KLIA                    | 79  |
| 3.10 | Cropped and geocoded unwrapped interferogram for KLIA (red box)  | 80  |
| 4.1  | Raw data for KLIA along with master image dated on 20070210  | 94  |
| 4.2  | Raw data for SCA along with master image dated on 20080208   | 95  |
| 4.3  | SLC data for KLIA and surrounding areas  | 97  |
| 4.4  | SLC data for SCA and surrounding area  | 97  |
| 4.5  | Generated interferograms for KLIA datasets   | 99  |
| 4.6  | Generated interferograms for SCA datasets  | 99  |
| 4.7  | Differential interferogram for KLIA after the removal of topography contribution                                   | 101 |
| 4.8  | Differential interferogram for SCA after the removal of topography contribution                                    | 102 |
| 4.9  | Coherence of all interferogram image pair for KLIA   | 103 |
| 4.10 | Coherence of all interferogram image pair for SCA  | 104 |
| 4.11 | The filtered interferogram pairs of KLIA using the Goldstein-Werner power-spectral filter                          | 106 |
| 4.12 | The filtered interferogram pairs of SCA using the Goldstein-Werner power-spectral filter                           | 107 |
| 4.13 | The unwrapped and geocoded interferograms of KLIA using coherence threshold of zero                                | 109 |
| 4.14 | The unwrapped and geocoded interferograms of KLIA using coherence threshold 0.1                                    | 111 |

|      |  |     |
|------|--|-----|
| 4.15 | The unwrapped and geocoded interferograms of KLIA using coherence threshold 0.2  | 112 |
| 4.16 | The unwrapped and geocoded interferograms of SCA using coherence threshold of zero   | 114 |
| 4.17 | The unwrapped and geocoded interferograms of SCA using coherence threshold 0.1   | 115 |
| 4.18 | The unwrapped and geocoded interferograms of SCA using coherence threshold 0.2   | 116 |
| 4.19 | The APS for KLIA by using ECMWF model  | 119 |
| 4.20 | The APS for SCA by using ECMWF model   | 120 |
| 4.21 | The interferograms pair of KLIA after the atmospheric correction by using ECMWF  | 122 |
| 4.22 | The interferograms pair of SCA after the atmospheric correction by using ECMWF   | 124 |
| 4.23 | The interferograms of KLIA after the orbital correction  | 127 |
| 4.24 | The interferograms of SCA after the orbital correction   | 129 |
| 4.25 | Google Earth image of KLIA with four zones; Runway 1 (Zone 1), Main Terminal (Zone 2), LCCT (Zone 3) and lastly, Runway 2 (Zone 4)                 | 131 |
| 4.26 | The time series deformation without atmospheric and orbital corrections of KLIA using coherence threshold value of 0.1 from 2007 until 2011        | 132 |
| 4.27 | The overlaid time series deformation map on Google Earth without atmospheric and orbital correction of KLIA using coherence threshold value of 0.1 | 133 |
| 4.28 | The time series deformation with atmospheric and orbital corrections of KLIA using coherence threshold value of 0.1 from 2007 until 2011           | 134 |
| 4.29 | The overlaid time series deformation map on Google Earth with atmospheric and orbital correction of KLIA using coherence threshold value of 0.1.   | 135 |
| 4.30 | Comparisons of time series deformation between   |     |

|      |   |     |
|------|---|-----|
|      | without (blue) and with (red) atmospheric and orbital error for Runway 1 (Zone 1)   | 137 |
| 4.31 | Comparisons of time series deformation between without (blue) and with (red) atmospheric and orbital error for Main Terminal (Zone 2)             | 138 |
| 4.32 | Comparisons of time series deformation between without (blue) and with (red) atmospheric and orbital error for LCCT (Zone 3)                      | 139 |
| 4.33 | Comparisons of time series deformation between without (blue) and with (red) atmospheric and orbital error for Runway 2 (Zone 4)                  | 140 |
| 4.34 | Google Earth image of SCA with three zones; Runway 2 (Zone 1), Terminal 1, 2, 3 (Zone 2) and Runway 1 (Zone 3)                                    | 141 |
| 4.35 | The time series deformation without atmospheric and orbital correction of SCA using coherence threshold value of 0.1 from 2007 until 2011         | 142 |
| 4.36 | The overlaid time series deformation map on Google Earth without atmospheric and orbital correction of SCA using coherence threshold value of 0.1 | 143 |
| 4.37 | The time series deformation with atmospheric and orbital correction of SCA using coherence threshold value of 0.1 from 2007 until 2011            | 144 |
| 4.38 | The overlaid time series deformation map on Google Earth with atmospheric and orbital correction of SCA using coherence threshold value of 0.1    | 145 |
| 4.39 | Comparisons of time series deformation between without (blue) and with (red) atmospheric and orbital error for Runway 2 (Zone 1)                  | 147 |
| 4.40 | Comparisons of time series deformation between without (blue) and with (red) atmospheric and orbital error for Terminal 1, 2, 3 (Zone 2)          | 148 |
| 4.41 | Comparisons of time series deformation between without (blue) and with (red) atmospheric and orbital  |     |

|      |  |     |
|------|--|-----|
|      | error for Runway 1 (Zone 3)  | 149 |
| 4.42 | Time series of land deformation at KLIA using MInTS  | 151 |
| 4.43 | The overlaid time series deformation map on Google Earth for KLIA by using MInTS technique               | 152 |
| 4.44 | Time series of land deformation at SCA using MInTS technique   | 153 |
| 4.45 | The overlaid time series deformation map on Google Earth for SCA by using MInTS technique                | 154 |
| 4.46 | Comparisons of time series deformation between SBAS (blue) and MInTS (red) for Runway 1 (Zone 1)         | 156 |
| 4.47 | Comparisons of time series deformation between SBAS (blue) and MInTS (red) for Main Terminal (Zone 2)    | 157 |
| 4.48 | Comparisons of time series deformation between SBAS (blue) and MInTS (red) for LCCT (Zone 3)             | 158 |
| 4.49 | Comparisons of time series deformation between SBAS (blue) and MInTS (red) for Runway 2 (Zone 4)         | 159 |
| 4.50 | Comparisons of time series deformation between SBAS (blue) and MInTS (red) for Runway 2 (Zone 1)         | 161 |
| 4.51 | Comparisons of time series deformation between SBAS (blue) and MInTS (red) for Terminal 1, 2, 3 (Zone 2) | 162 |
| 4.52 | Comparisons of time series deformation between SBAS (blue) and MInTS (red) for Runway 1 (Zone 3)         | 163 |

## LIST OF SYMBOLS

|                     |   |
|---------------------|---|
| $\Delta\phi_{topo}$ | phase contribution from topographic phase   |
| $\Delta\phi_{defo}$ | phase contribution from some motion or deformation of the surface                   |
| $\Delta\phi_{flat}$ | phase contribution from the flat term   |
| $B_n$               | perpendicular baseline  |
| $B_p$               | parallel baseline   |
| $B_{\perp}$         | perpendicular baseline  |
| $\Phi_{ij}$         | pixel phase of the interferogram combining acquisition $i$ and $j$                  |
| $L^0$               | minimum spanning tree   |
| $L^1$               | minimum cost flow   |
| $R_1$ and $R_2$     | distance between the satellite and the target,                                      |
| $R_d$               | dry air specific gas constants (287.05 J.kg <sup>-1</sup> .K <sup>-1</sup> )        |
| $R_v$               | water vapour specific gas constants (461.495 J. kg <sup>-1</sup> .K <sup>-1</sup> ) |
| $S_1$ and $S_2$     | complex SAR images  |
| $S_k(i, j)$         | complex value of the master ( $k = 1$ ) or slave ( $k = 2$ ) scene pixel ( $i, j$ ) |
| $W_{ij}^{mn}$       | particular wavelet coefficient with index $mn$ in interferogram $ij$                |
| $d_{ij}(x, y)$      | value of the pixel at range $x$ and azimuth $y$                                     |
| $g_m$               | weighted average of the gravity acceleration between $z$ and $z_{ref}$              |
| $u_i$               | column vectors of U (M x M orthogonal matrix)                                       |
| $v_i$               | column vectors of U V(N x M orthogonal matrix)                                      |

|                    |   |
|--------------------|---|
| $Z_{ref}$          | reference altitude  |
| $\delta L_{LOS}^S$ | LOS single path delay   |
| $\delta\phi_n$     | pixel phase increment between acquisition time $n$ and $n + 1$    |
| $\rho_1$           | distance between satellite antenna and the pixel                  |
| $\sigma^o$         | backscattering coefficient  |
| $\omega_1$         | unknown phase due to the interaction of the wave and the ground   |
| $\omega_{mn}$      | reference frame shift for the interferogram                       |
| $\phi_{atmos}$     | phase contribution due to atmospheric phase delay                 |
| $\phi_{path}$      | phase contribution due to path length                             |
| $\phi_{pixel}$     | phase contribution due to individual scatterers within SAR pixels |
| $\Delta\rho$       | cross-track slant range   |
| $\Delta\phi$       | phase different   |
| $c$                | speed of light  |
| $e$                | altitude ambiguity  |
| $e$                | water vapour partial pressure in Pa,                              |
| $h$                | terrain height  |
| $H$                | spacecraft height   |
| $I(i, j)$          | interferogram phase of the $(i, j)$ pixel and                     |
| $L$                | length of radar antenna   |
| $N$                | geoid separation  |
| $P$                | dry air partial pressure in Pa                                    |
| $Q(u, v)$          | filter response   |
| $R$                | range   |
| $T$                | temperature in K  |
| $t$                | time  |
| $Z(u, v)$          | Fourier transformation of interferometric phase                   |
| $\Delta R$         | slant range resolution  |
| $\Delta\theta$     | look angle  |
| $\alpha$           | horizontal baseline angle   |
| $\alpha$           | filter parameter between zero and one                             |
| $\beta$            | radar bandwidth   |

|              |   |
|--------------|---|
| $\gamma$     | coherence                                   |
| $\delta\phi$ | phase corrected for the curved Earth effect |
| $\theta$     | off nadir radar look angle                  |
| $\theta$     | look angle                                  |
| $\lambda$    | wavelength                                  |
| $\pi$        | constant(3.142)                             |
| $\rho$       | nominal slant range                         |
| $\tau$       | pulse length                                |
| $\phi$       | phase                                       |

## LIST OF ABBREVIATIONS

|         |  |
|---------|--|
| 2D      | 2 Dimensional  |
| 3D      | 3 Dimensional  |
| ALOS    | Advanced Land Observing Satellite                    |
| APS     | Atmospheric Phase Screen                             |
| ASAR    | Advanced Synthetic Aperture Radar                    |
| AUIG2   | ALOS- PALSAR-2/ALOS PALSAR User Interface Gateway    |
| CPT     | Coherent Pixels Technique                            |
| DEM     | Digital Elevation Model                              |
| DInSAR  | Differential InSAR                                   |
| DORIS   | Delft Object-Oriented Radar Interferometric Software |
| DWT     | Discrete Wavelet Transforms                          |
| EB      | Evidential Belief                                    |
| ECMWF   | European Center for Medium range Weather Forecasting |
| ENVISAT | Environmental Satellite                              |
| ERA-I   | European Center for Medium-Range Weather Forecast    |
| ERS     | European Remote Sensing Satellite                    |
| FBD     | Fine Beam Dual Polarization                          |
| FBS     | Fine Beam Single Polarization                        |
| FM      | Frequency Modulation                                 |
| FR      | Frequency ratio                                      |
| FWT     | Fast Wavelet Transform                               |
| GAM     | Global Atmospheric Models                            |
| GIAnt   | Generic InSAR Analysis Toolbox                       |
| GPS     | Global Positioning System                            |
| HDF     | Hierarchical Data Format                             |

|          |   |
|----------|---|
| HKIA     | Hong Kong International Airport                                 |
| InSAR    | Spaceborne Interferometric Synthetic Aperture Radar             |
| ISBAS    | Intermittent Small Baseline Subset                              |
| ISCE     | InSAR Scientific Computing Environment                          |
| IWT      | Inverse Wavelet Transform                                       |
| JAXA     | Japan Aerospace and Exploration Agency                          |
| JERS     | Japan Earth Resources Satellite                                 |
| JPL      | Jet Propulsion Laboratory                                       |
| KLIA     | Kuala Lumpur International Airport                              |
| LCCT     | Low cost carrier terminal                                       |
| LOS      | Line-Of-Sight   |
| LS       | Least Square  |
| MAI      | Multiple Aperture Interferogram                                 |
| MERIS    | Medium Resolution Imaging Spectrometer Instrument               |
| MERRA    | Modern Era Retrospective-Analysis for Research and Applications |
| MInTS    | Multiscale InSAR time series                                    |
| MM5      | Mesoscale Meteorological Model                                  |
| MODIS    | Moderate Resolution Imaging Spectroradiometer                   |
| MT-InSAR | Multi-temporal InSAR  |
| NARR     | North American Regional Reanalysis                              |
| NASA     | National Aeronautics and Space Administration                   |
| NSBAS    | New-SBAS  |
| PALSAR   | Phased Array type L-band Synthetic Aperture Radar               |
| PolSAR   | Polar-orbiting satellite  |
| PS       | Permanent Scatterers  |
| PSI      | Persistent Scatterer Interferometry                             |
| PyAPS    | Python Atmospheric Phase Screen                                 |
| Radar    | Radio Detection and Ranging                                     |
| RADARSAT | RADAR SATellite   |
| RMS      | Root mean square  |
| ROC      | Rate of Change  |
| SAR      | Synthetic Aperture Radar  |
| SB       | Small Baseline  |

|        |  |
|--------|--|
| SBAS   | Small Baseline Subset  |
| SCA    | Singapore Changi Airport   |
| SCH    | S is the local along track direction, C is the cross track direction, and H is the height above the approximating sphere |
| SEASAT | Sea Satellite  |
| SLC    | Single Look Complex  |
| SNAPHU | Statistical-cost, Network-flow Algorithm for Phase Unwrapping  |
| SNR    | Signal Noise Ratio   |
| SRTM   | Shuttle Radar Topography Mission   |
| StaMPS | Stanford Method for Persistent Scatterers  |
| SVD    | Singular Value Decomposition   |
| TEC    | Total Electron Content   |
| UK     | United Kingdom   |
| WGS    | World Geodetic System  |

**LIST OF APPENDICES**

- Appendix A**            The interferograms pair of KLIA after atmospheric correction by using ECMWF for coherence threshold limit zero (0)
- Appendix B**            The interferograms pair of KLIA after atmospheric correction by using ECMWF for coherence threshold limit 0.2
- Appendix C**            The interferograms pair of SCA after atmospheric correction by using ECMWF for coherence threshold limit zero (0)
- Appendix D**            The interferograms pair of SCA after atmospheric correction by using ECMWF for coherence threshold limit 0.2
- Appendix E**            The interferograms pair of KLIA after the orbital correction for coherence threshold zero (0)
- Appendix F**            The interferograms pair of KLIA after the orbital correction for coherence threshold 0.2
- Appendix G**            The interferograms pair of SCA after the orbital correction for coherence threshold zero (0)
- Appendix H**            The interferograms pair of SCA after the orbital correction for coherence threshold 0.2

## **CHAPTER 1**

### **INTRODUCTION**

This chapter explores the background of the study, problem statement and research objectives. It describes in brief the significance of this research and the outline of this thesis.

#### **1.1 Background of the Study**

Over the last few decades, land subsidence has become a global problem due to several factors like groundwater extraction, sinkhole or underground mine collapse, rapid land development, natural hazard and so on (Zizzi, 2013). This phenomenon can take place slowly, becoming evident over a time span of many years, where the land surface starts to subside and sink due to either geological or human activities (Liu *et al.*, 2008). Land subsidence can lead to great economic losses (Motagh *et al.*, 2007; Liu *et al.*, 2008) and many other problems, including changes in elevation; damage to structures such as storm drains, sanitary sewers, roads, railroads, canals, levees, bridges, public and private buildings and so on. Additionally, land subsidence may cause serious harm to flood control drainage, land

use, urban planning, construction and transportations (Zhou and Zhao, 2013). The increasing development of land plays an important role in occurring land subsidence around the world. Abidin *et al.* (2009) discussed the relation between land subsidence and urban development activities and found that the spatial and temporal variations of land subsidence depend on the corresponding variations of groundwater extraction, coupled with the characteristics of sedimentary layers and building loads.

Land subsidence associate with groundwater level decline has been recognized as a potential problem in various parts of the world. Important cities such as London, Venice, Mexico, Jakarta, Tokyo, *etc.*, have experienced land subsidence due to over-extraction of groundwater for domestic and industrial purposes (Sahu and Sikdar, 2011). Most cities usually have big infrastructures like bridges, tunnels, highways, railways, airports, seaports, power plants, dams, wastewater projects, oil and natural gas extraction projects, public buildings, information technology systems, aerospace projects, and weapons systems (Gupta *et al.*, 2009). These infrastructures on the land are most likely to subside due to several factors especially the ability of the land to accommodate the pressure from the big infrastructures. For example, Mexico City has sunk about 30 feet in the last century due to its exponential growth (Huby, 2001) and severe land subsidence due to consolidation of the lacustrine aquitard caused by aquifer exploitation (Ortega-Guerrero *et al.*, 1999).

Monitoring land subsidence is very crucial especially in area where massive infrastructures have been developed in order to carry out different kinds of activities. Several methods are used to monitor the land subsidence, including levelling, total station survey, and Global Positioning System (GPS) field survey. Levelling survey has been traditionally used for monitoring the land subsidence (Odijk *et al.*, 2003) but this technique is expensive and time consuming since it requires a lot of field workers and only allows detection of subsidence over a very small area (Strozzi *et al.*, 2001). Moreover, the precise levelling is usually required a wide network of benchmark for the subsiding area. The used of total station is commonly seen since this method can maintain the considerable accuracy for many public works such as road, airport and city (Lee and Rho, 2001). Both levelling survey and total stations

survey can deliver 0.1mm height change accuracy (Ge *et al.*, 2004). Besides that, GPS is also used to detect deformation with millimeter to centimeter accuracy on localized areas (Cao *et al.*, 2008). However, GPS observations require logging times from one to several hours for each baseline to achieve high precision. This expenditure is also highly time consuming and impracticable for many engineering works and ground reconnaissance survey (Gili *et al.*, 2000).

Spaceborne Interferometric Synthetic Aperture Radar (InSAR) is a valuable technique for measuring surface deformation which has been introduced more than a decade ago and has become an important part of deformation monitoring (Hooper, 2008; Samsonov *et al.*, 2010). The technique of InSAR relies on combining phase information from two or more SAR acquisition of the same area captured at different times from a similar platform to produce an interferogram (Massonet and Feigl, 1998). This process shows range changes in the view direction between the platform and the Earth's surface, and can be further proceed with a topographic model to detect ground deformation up to cm or sub-cm level of precision (Massonet, 2008; Samsonov *et al.*, 2010; Liu *et al.*, 2014). InSAR offers the typical advantages like data acquisition over inaccessible areas, wide area coverage, its competitive cost, data availability, and its high vertical accuracy for remotely measuring the deformation of the ground and manmade structures from space (Crosetto *et al.*, 2008; Simon and Rosen, 2007).

Nevertheless, the InSAR phase is sensitive to the terrain topography and relative changes in the elevation occurring between two SAR antenna passes over the same area. If the terrain topography of the images scene are available, *i.e.* a DEM (Digital Elevation Model), the corresponding phase component can be subtracted from the InSAR phase, leaving the component due to the terrain surface deformation is a process called Differential InSAR (DInSAR) technique (Fan *et al.*, 2011). DInSAR technique provide high resolution ground deformation at regional level along the line-of-sight direction between the satellite antenna and the ground surface by exploiting the phase difference between two time-separated complex SAR image acquired under similar geometric condition (Massonet *et al.*, 1993,1995; Amelung *et*

*al.*, 2000; Fialko *et al.*, 2005; Shankar, 2013). It has been widely used in a number of types of applications like earthquake displacement (Massonet *et al.*, 1993), volcano deformation (Massonet *et al.*, 1995), glacier dynamics (Goldstein *et al.*, 1993; Joughin, 1996, Mohr *et al.*, 1998), and land subsidence (Strozzi and Wegmuller, 1999; Strozzi *et al.*, 1999; Fruneau *et al.*, 1999; Ferretti *et al.*, 1999; Strozzi *et al.*, 2000) considering its usefulness to monitor land subsidence effectively over the conventional InSAR technique.

Despite the successful use of InSAR/DInSAR technique for the deformation monitoring, the limitation as well as the complexity of the processing for this technology should not be taken lightly. The complexity of the processing include several steps of computation such as baseline estimation, focusing, coregistration, generation of interferogram, filtering and phase unwrapping which need to be performed carefully based on the data and type of surface feature under investigation. Besides, this technique is highly sensitive to atmospheric conditions (Wegmuller *et al.*, 2006; Meyer *et al.*, 2006; Chen and Zebker, 2012; Chapin *et al.*, 2006; Jung *et al.*, 2013) and orbital errors (Kohlhase *et al.*, 2003; Shirzaei and Walter, 2011; Liu *et al.*, 2014). The orbit influence can easily be distinguished from deformation influences but that error makes the interferogram look sloped and the deformation spots often cannot be recognized (Capková, 2005). Since satellite propagates the signals through the atmosphere, the signal might either have propagation delay or bending effect (Rosen *et al.*, 2000; Ding *et al.*, 2004; Balaji, 2011). However, most of the signals have the propagation delay because of the effect from the troposphere and ionosphere which are known as the main error in atmosphere (Ferretti *et al.*, 2001; Mora *et al.*, 2003; Werner *et al.*, 2003; Hooper *et al.*, 2004; Lanari *et al.*, 2004; Kampes, 2006; Chen and Zebker, 2012).

Recent development of numerous algorithms that combine phase information from multiple radar interferograms and produce internally consistent time-series of land surface deformation have the ability to overcome atmospheric as well as the orbital errors (Ferretti *et al.*, 2001; Berardino *et al.*, 2002; Hetland *et al.*, 2012). Combining multiple interferogram allows detection and quantification of both

secular and transient displacement and these methods also help to mitigate the effects of change in scatterer properties and phase delay introduced by the orbit and atmosphere between SAR acquisitions, resulting in measurements of surface deformation with subcentimeter accuracy (Hanssen and Klees, 1998; Bürgmann, 2000; Hetland *et al.*, 2012). Many efforts have been made to minimize troposphere error such as by computing the phase delay using global meteorological reanalysis data (Jolivet *et al.*, 2011), using wavelet transform (Shirzaei and Burgmann, 2012), formation of atmospheric model (Wadge *et al.*, 2002), and atmospheric phase screen filters (Puysegur *et al.*, 2007). Efforts have also been made to remove orbital error using a bilinear or biquadratic model (Amelung *et al.*, 2007), using a function in terms of the standard deviation of the velocity gradient in range and azimuth direction, (Fattahi and Amelung, 2014), using wavelet multiresolution analysis and robust regression approach (Shirzaei and Walter, 2011).

Nevertheless, the conclusion can be drawn from the above background information is that monitoring land subsidence is important and it can be done using InSAR technique although several limitations of this approach have been highlighted in the literatures. The use of time series InSAR technique is surely an attractive approach to measure the land subsidence which can incorporate several SAR interferograms and techniques to overcome atmospheric disturbance and the orbital decorrelation. Despite, the results of accurate measurements for land deformation from previous study demonstrated the usefulness of the InSAR time series approach for different types of land surfaces. However, hardly any study can be seen in the literature where this time series approach has been used to monitor big infrastructures such as airport although massive infrastructural development has been occurred in the airport area.

## 1.2 Problem Statement

It is overwhelmingly that land subsidence is a severer threat to large infrastructures such as buildings, dams, bridges, roads, and so on. Similar to the other infrastructures, airport, which is considered as the centre of the modern communication system, is susceptible to have land subsidence problem due to several reasons (Liu *et al.*, 2001; Jiang and Lin, 2010; Zhao *et al.*, 2011). Monitoring the subsidence of airport is important, not only considering the sustainability of the infrastructure but also in order to prevent undesirable loss of property and life because subsidence can cause severe accident during take-off and landing of airplanes. Remote sensing techniques specifically InSAR technique can be used to monitor land subsidence at airport with high spatial accuracy. Several studies have successfully demonstrated the capability of InSAR to monitor the land subsidence at airport but most of the studies investigation focused on airports that are built on the reclaimed land (Liu *et al.*, 2001; Ding *et al.*, 2004; Zhao *et al.*, 2011) or high latitude permafrost environment (Short *et al.*, 2014). Nevertheless, there are many airports that have not been developed on the reclaimed lands but can still be affected by the land subsidence due to natural or human activities especially underground water or hydrocarbon extraction (Ding *et al.*, 2004; Aly *et al.*, 2009; Bhattacharya, 2013), therefore, the airports area need to be investigated with an effective monitoring system in order to monitor the sustainability.

Kuala Lumpur International Airport (KLIA) and Singapore Changi Airport (SCA) are the two busiest airports in the South East Asia region and these airports are the main airport of Malaysia and Singapore respectively. KLIA was built in 1998 with an area about 100km<sup>2</sup> on an agricultural land which has the capacity to handle 70 million passengers and 1.2 million tonnes of cargo per year (Airports-Worldwide, 2004). On the other hand, SCA airport was built in 1981 at the eastern tip of the main island at Changi, where the airport would easily be expanded through land reclamation. It is about 17.2 km northeast from the commercial centre in Changi, on a 13km<sup>2</sup> site (Bonny, 2001). KLIA is 16 year old and due to the rapid pace of development, parts of Malaysia, especially in the Kuala Lumpur, have experienced

unprecedented growth rates with development areas increasing and because of the shortage of land, the city is expanded over high-risk ground, such as hilly terrain, areas with karstic bedrock, ex-mining land, peat and soft sediment areas. The existences of geohazards such as landslides and sinkholes have affected the urban dwellers (Chand, 1998). Besides that, SCA is a hydraulic sand filled project with associated soil improvement works and this man-made structure is still in expanded process from time to time due to high demands for air travel that expected to grow in the coming years (Choa, 1994). However, although these two airports are the busiest airport in the world, more than one decade old and several extending work have been done, no robust system have been developed to monitor the land deformation as well as the infrastructural sustainability especially using InSAR technique.

Indeed, monitoring the land subsidence of airport using InSAR technique is an attractive approach but this technique is not easy to implement without an appropriate data processing strategy in order to get better estimation accuracy. However, in general, the difficulties of InSAR data processing can be seen with respect to few perspectives which includes i) baseline determination, ii) co-registration, iii) coherence determination, iii) interferogram generation, iv) interferogram filtering, v) phase unwrapping (Zebker *et al.*, 1992), as there is no clear cut rule that can be followed for each processing step. As a matter of fact, the five aforementioned processing steps are mostly relied on several factors such as sensor and wavelength, data availability, types of land feature/target under investigation, accuracy requirement, and availability of the required software or algorithm.

Nevertheless, other than the SAR processing problem, an interferogram contain four error components due to orbital error, residual topography error, atmospheric noise (mainly tropospheric artefact) and decorrelation noise (Zebker *et al* 1997; Hanssen, 2001; Puyseegur *et al.*, 2007; Liu *et al.*, 2014). Although some errors such as topographic error and decoloration error can be reduced systematically, atmospheric noise (tropospheric artefact) and orbital errors are the major source of error in the SAR data that need to be treated carefully. The

troposphere contains approximately 75% of the atmosphere's mass and 99% of its water vapour and aerosol (Meteoblue, 2006). The major contribution to the phase delay is the highly variable water vapour content in the troposphere (Lofgren *et al.*, 2010). The spatial and temporal variability of tropospheric water vapour modifies the refractivity of radio wave passing between satellite and the ground (Wadge *et al.*, 2002; Jolivet, 2011). The pattern and amplitude of the atmospheric phase delay shows limitation on the measurement of low amplitude and large spatial wavelength signal related to interseismic deformation (Wright *et al.*, 2004). Besides that, the orbital error is considered as the main limitation in InSAR. The variations in the radial and cross-track components of the orbital error during the SAR acquisition generate the orbital fringes, the so-called phase ramp, which is often parallel to the satellite track and may also generate the perpendicular fringes (Hanssen, 2001). In order to reduce the effects of orbital error, for the case of topography height estimation, tie points or ground control points can be used to constrain the reference phase at certain points in each interferogram (Massonnet and Feigl, 1998; Hanssen, 2001; Lundgren *et al.*, 2009)

Multi temporal InSAR technique is an extension of InSAR that use large sets of SAR scenes to investigate the temporal evolution of deformation and mitigate errors found in single interferograms (Wortham, 2014). Stacking or averaging of interferograms is the simplest form of multi temporal processing (Sandwell and Price, 1998) which assumes that the deformation is linear, and uses the stack average to estimate a constant deformation rate. Other multi-temporal approaches include Persistent Scatterer InSAR (PS-InSAR) technique (Ferreti *et al.*, 2001; Werner *et al.*, 2003; Hooper *et al.*, 2004) which analyses the temporal signal on specific targets and small baseline (SB) (Berardino *et al.*, 2002; Mora *et al.*, 2003) technique which selects the most reliable pairs according to temporal and spatial baselines. Other than that, another multi-temporal technique proposed by Hetland *et al.* (2012) called as Multiscale InSAR time series (MInTS) which is based on wavelet decomposition of the interferogram in space and a general parametrization in time is a new multi temporal approach to extracting spatially and temporally continuous ground deformation from InSAR data (Agram, 2013).

Therefore, considering the several issues in the problem statement such as i) the necessity of monitoring land subsidence/land deformation of these two busiest airports, ii) the effectiveness of InSAR time series techniques especially SBAS and MInTS for the estimation of land subsidence/land deformation, iii) lack of investigations in the literature for monitoring land subsidence/land deformation using InSAR technology especially in the study areas, and iv) availability of long-term SAR data from different satellite sensors, this research is going to take an opportunity to study long term (2007-2011) land subsidence/land deformation at the KLIA and SCA using data from ALOS PALSAR satellite. Removal of atmospheric artificial and orbital error from the interferogram and the estimation of displacement were done using SBAS and MInTS techniques.

### **1.3 Research Objectives**

The overall objective of this research is to monitor the long term land surface deformation at KLIA and SCA using time series InSAR techniques. The sub-objectives of this research are listed as below:

1. To examine the impact of atmospheric (tropospheric) as well as orbital correction on the improvement of land deformation estimation accuracy
2. To compare the results of the land surface deformation between two different time series InSAR techniques which is SBAS and MInTS
3. To investigate the deformation pattern of the airports which was built on two different types of land which is in agricultural land (KLIA) and reclaimed land (SCA)

Regarding to objective one, the research questions are as follows:

- 1 How much is the impact of tropospheric and orbital errors on the land subsidence estimation?
- 2 What is the different of land subsidence estimation before and after both corrections are going to be applied?

Regarding to objective two, the research questions are as follows:

1. What are the different of land subsidence measurements obtained using these two techniques?
2. Which technique is the most stable for land surface deformation monitoring?

Regarding to objective three, the research question are as follows:

1. Do the different types of land uses affect the land subsidence at the KLIA and SCA?

#### 1.4 Scope of the Study

1. This study used SAR data since it has wide application in mapping of the surfaces of the Earth as well as monitoring ground subsidence from a variety of causes, in particular subsidence due to water extraction from underground reservoirs and subsidence in reclaimed land.
2. A long-term data were obtained in order to study the long-term deformation in the study areas. The data from ALOS PALSAR sensor were downloaded and used for this study as these sensors can provide data with reasonable spatial and temporal resolution.
3. KLIA and SCA have been chosen as the area of interest since these two airports are the most important infrastructures for both countries in context of communication, business, and social connection.
4. Due to its availability and the satellite revisit time at the study areas, the SAR data from 2007-2011 were used for both study sites which are KLIA and SCA. Start with 15 SAR raw data for KLIA and 14 SAR raw data for SCA, the data were processed using in order to generate DInSAR and further were continued to estimate the land subsidence at both study area.
5. An external data like Digital Elevation Model (DEM) were used to generate interferogram using DInSAR technique. Shuttle Radar Topography Mission (SRTM) (~90 m) data were used and this DEM data is free and spatial coverage is available for the study areas.

6. Generation of differential interferogram which involves focusing, coregistration, interferogram and coherence generation, filtering, phase unwrapping and geocoding were first done using InSAR Scientific Computing Environment (ISCE) software because it offers to the scientific community an open-source, modular and extensible computing environment.
7. After the interferogram were unwrapped, the atmospheric correction were applied to the unwrapped interferogram by using atmospheric weather model *i.e.* European Center for Medium range Weather Forecasting (ECMWF)
8. After the atmospheric correction was applied to each unwrapped interferogram, the orbital effects on interferograms were estimated independently using the network de-ramping method.
9. Time series estimation of land subsidence from the interferogram using 1) SBAS where data pairs were characterized by small spatial and temporal separation between acquisitions and 2) MInTS which operates in the spatial wavelet domain were used
10. Both atmospheric and orbital error corrections and also the deformation detection for both study area were processed in software named Generic InSAR Analysis Toolbox (GIANt).

## 1.5 Study Area

In this study, two study sites were examined in order to evaluate the land subsidence measurement. As can be seen in Figure 1.1, the first selected study site is the KLIA (02°44'36"N, 101°41'53"E) located in the Langat Basin. Langat basin can be divided into 3 distinct zones; the mountainous zone of the northeast corner of Hulu Langat district, the hilly area characterized by gentle slopes spreading widely from north to the east in the middle part of Langat basin and third zone is a relatively flat alluvial plane located in the southwest of Langat Basin (Idrus, 2004).

KLIA is the main and largest airport in Malaysia with an area about 100 km<sup>2</sup>. KLIA was opened officially on June 27, 1998. It is designed and built to be an efficient, competitive and world-class airport for the Asia-Pacific Region (Airports-Worldwide, 2004). KLIA is completed with the latest technology and state-of-the-art facilities, aims at providing maximum passenger safety, comfort and convenience. It is a unique airport which has facility for business, entertainment and relaxation.

Moreover, it is important to note that it was built on agricultural land which was used before for rubber and palm oil plantations and Langat Basin has a history of groundwater extraction (Bringemeier, 2001). Based on the results of the detailed hydrogeological, geophysical exploration and numerical groundwater modelling, the fractured, jointed and partially weathered meta-sandstone beds forming the Palaeozoic basement rocks at KLIA and KLIA2 has been identified as potentially productive fractured rock aquifers.

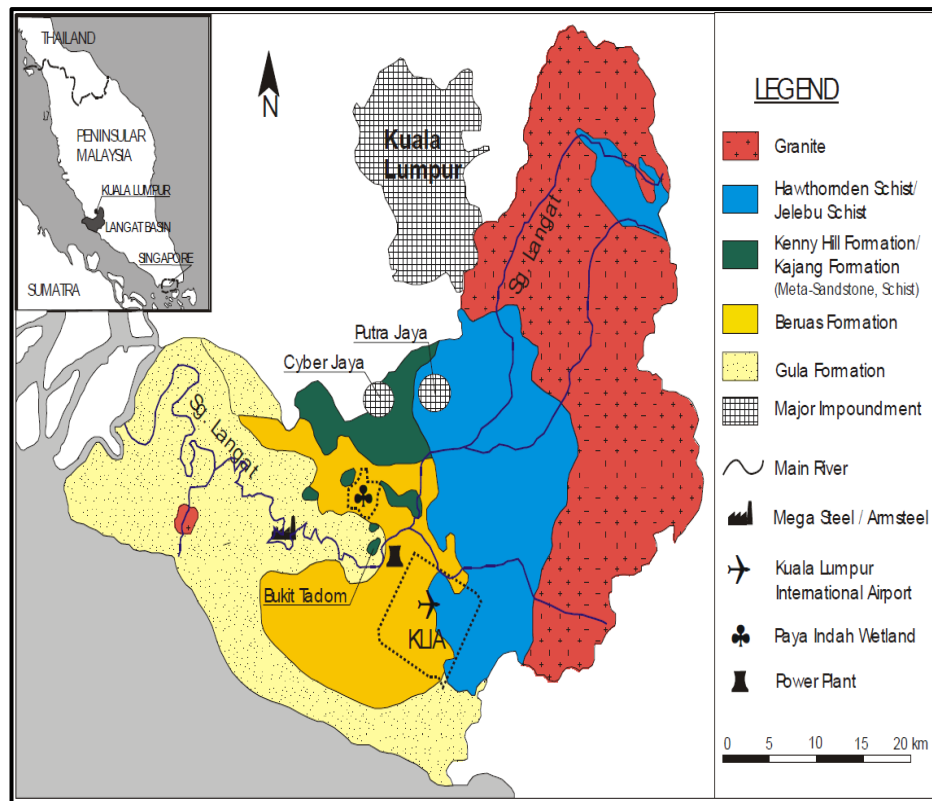


**Figure 1.1** Map of Langkat Basin (Source: Bringemeier, 2001)

The other selected study site is the SCA (Figure 1.2) which indeed the world's most highly acclaimed airports (Park, 1997). It was opened in 1981 with a design capacity of 12 million passengers a year. It is located about 17.2 km northeast from the commercial center in Changi, on a 13 square kilometres site. It has three passenger terminals with a total annual handling capacity of 66 million passengers (Bonny, 2001).

This airport could claim to be the region's first real international hub, being strategically located at the crossroads between Europe and the Far East, and the Far East and Australasia (Paylor, 1994). It is one of the largest single development projects in Singapore's history and was built in reclaimed land. The land reclamation work is a process of placing fill geomaterials on existing geological formations over a large extent. The geological conditions will significantly affect the planning, design and implementation of a land reclamation and ground improvement project (Bo and Chu, 2006). For Changi Airport, the land-reclamation was carried out to

extend the land at the foreshore of the eastern part of Singapore. The area reclaimed is about 2000 hectares and it is used for the airport runway, taxiways and the terminal buildings. The depth of seabed at the reclamation area ranges between 2 metres and 15 metres being much deeper at the northern edge of the area (Arulrajah, 2008).



**Figure 1.2** Singapore Changi Airport (red circle) which built on reclaimed land (Source: Utehas, 2016)

## 1.6 Significance of the Study

Monitoring of land subsidence is crucial for several purposes include avoiding unwanted damage of property and loss of valuable life. Airport is a big infrastructure where thousands of people are gathered together and used hundreds of flight in order to perform the valuable journey from one place to another place.

Ground surface of an airport especially the runway is very important and sensitive part. Any unexpected land subsidence at the runway or ground surface can cause severe threat to human life and property. Therefore, an airport needs to be monitored for land subsidence with an effective technique.

This study is going to find out an efficient technique for the monitoring of land subsidence of two busiest airports in Southeast Asian region, hence, undoubtedly this research is important and would be beneficial for Malaysia and Singapore and also for several agencies, in particular for those who are interested in land subsidence monitoring. Some of the specific significance of this study can be highlighted as follows:

- 1 As a new technique, the result can be very useful to improve the monitoring system of airport in Malaysia and Singapore and can obtain a great level of accuracy.
- 2 It can improve capability to predict future subsidence in new area or in the existing land subsidence areas at the airports.
- 3 This study would be very helpful for the airport management in order to detect the potential location of suspected subsidence area.
- 4 The method will be very useful source for any agencies who are interested to apply this method for the other airports or other infrastructures in Malaysia and Singapore.
- 5 As a reference for future research to explore more about InSAR technique for other purposes like landslide which occurs frequently in Malaysia.

## 1.7 Thesis Outline

This thesis has been divided into six chapters which are as follows:

**Chapter 1** provides general overview of the main topic of this research work, problem statement, research identification which includes research aim, objective and research questions, scope of the study, study area and significance of the study.

**Chapter 2** provide a literature review on related works including the InSAR technique, error in InSAR data like tropospheric and orbital effects, the used of SBAS and MInTS technique and also previous method used in order to correct both effects and the land subsidence monitoring at airports.

**Chapter 3** the methodology and details about the data processing and datasets are explained. The parameters related to this topic are described and advantages and disadvantages for the chosen method are stated in this chapter.

**Chapter 4** the results and analysis of the processing were shown which include the DInSAR generation, the corrected interferogram after the tropospheric and orbital correction were applied and the time series results for both technique.

**Chapter 5** the overall process from the start to end and the possible reasons for what is happening based on the results were discussed.

**Chapter 6** the conclusion and recommendation for this thesis were drawn.

## REFERENCES

- Abdelfattah, R. (2009). *InSAR phase analysis: Phase unwrapping for noisy SAR interferograms*. INTECH Open Access Publisher.
- Abidin, H. Z., Andreas, H., Gumilar, I., Sidiq, T. P., Gamal, M., Murdohardono, D., and Supriyadi, Y. F. (2010). Studying land subsidence in Semarang (Indonesia) using geodetic methods. In *FIG Congress, Facing the Challenges—Building the Capacity, Sydney, Australia*.
- Abidin, H. Z., Andreas, H., Kato, T., Ito, T., Meilano, I., Kimata, F., and Harjono, H. (2009). Crustal deformation studies in Java (Indonesia) using GPS. *Journal of Earthquake and Tsunami*, 3(02). 77-88.
- Agram, P. S., Jolivet, R., Riel, B., Lin, Y. N., Simons, M., Hetland, E., and Lasserre, C. (2013). New radar interferometric time series analysis toolbox released. *Eos, Transactions American Geophysical Union*, 94(7). 69-70.
- Agram, P., Jolivet, R., Simons, M., and Riel, B. (2012). GIAN-T-Generic InSAR Analysis Toolbox. In *AGU Fall Meeting Abstracts*. 1,0897.
- Ai, B., Liu, K., Li, X., and Li, D. H. (2008). *Flat-earth phase removal algorithm improved with frequency information of interferogram*. In *Geoinformatics 2008 and Joint Conference on GIS and Built Environment: Classification of Remote Sensing Images* (pp. 71471A-71471A). International Society for Optics and Photonics.
- Airports-Worldwide (2004), retrieved on 4 June 2014 from [http://www.airports-worldwide.com/malaysia/kuala\\_lumpur\\_intl\\_malaysia.php](http://www.airports-worldwide.com/malaysia/kuala_lumpur_intl_malaysia.php)
- Aly, M. H., Zebker, H. A., Giardino, J. R., and Klein, A. G. (2009). Permanent Scatterer investigation of land subsidence in Greater Cairo, Egypt. *Geophysical Journal International*, 178(3). 1238-1245.

- Amelung, F., Oppenheimer, C., Segall, P., and Zebker, H. (2000). Ground deformation near Gada 'Ale Volcano, Afar, observed by radar interferometry. *Geophysical research letters*, 27(19). 3093-3096.
- Amelung, F., Yun, S. H., Walter, T. R., Segall, P., and Kim, S. W. (2007). Stress control of deep rift intrusion at Mauna Loa volcano, Hawaii. *Science*, 316(5827). 1026-1030.
- Aobpaet, A., Cuenca, M. C., Hooper, A., and Trisirisatayawong, I. (2013). InSAR time-series analysis of land subsidence in Bangkok, Thailand. *International Journal of Remote Sensing*, 34(8). 2969-2982.
- API (2015) retrieved on 31 January, 2015 from <http://www.pybytes.com/pywavelets/ref/idwt-inverse-discrete-wavelet-transform.html>
- Arangio, S., Calò, F., Di Mauro, M., Bonano, M., Marsella, M., and Manunta, M. (2014). An application of the SBAS-DInSAR technique for the assessment of structural damage in the city of Rome. *Structure and Infrastructure Engineering*, 10(11), 1469-1483.
- Arnaud, A., Adam, N., Hanssen, R., Inglada, J., Duro, J., Closa, J. and Eineder, M., (2003). ASAR ERS interferometric phase continuity. In *Geoscience and Remote Sensing Symposium, 2003. IGARSS'03. Proceedings. 2003 IEEE International* (Vol. 2, pp. 1133-1135).
- Arulrajah, A., Bo, M. W., and Nikraz, H. (2008). Case Study of the Changi East Land Reclamation Project, Singapore.
- ASF (2016) retrieved on 4 March 2016 from <https://www.asf.alaska.edu/sar-data/insar/>
- Bähr, H., and Hanssen, R. F. (2012). Reliable estimation of orbit errors in spaceborne SAR interferometry. *Journal of Geodesy*, 86(12), 1147-1164.
- Balaji, P. M. (2011). Estimation and Correction of Tropospheric and Ionospheric Effects on Differential SAR Interferograms. *M. Sc., Indian Institute of Remote Sensing (IIRS) and International Institute for Geoinformation Science and Earth Observation (ITC)*.
- Bamler, R., and Hartl, P. (1998). Synthetic aperture radar interferometry. *Inverse problems*, 14(4). R1.
- Baran, I., Stewart, M. P., Kampes, B. M., Perski, Z., and Lilly, P. (2003). A modification to the Goldstein radar interferogram filter. *IEEE Transactions on Geoscience and Remote Sensing*, 41(9). 2114-2118.

- Bateson, L., Cigna, F., Boon, D., and Sowter, A. (2015). The application of the Intermittent SBAS (ISBAS) InSAR method to the South Wales Coalfield, UK. *International Journal of Applied Earth Observation and Geoinformation*, 34, 249-257.
- Bayuaji, L., Sumantyo, J. T. S., and Kuze, H. (2010). ALOS PALSAR D-InSAR for land subsidence mapping in Jakarta, Indonesia. *Canadian Journal of Remote Sensing*, 36(1). 1-8.
- Bechor, N. B., and Zebker, H. A. (2006). Measuring two-dimensional movements using a single InSAR pair. *Geophysical research letters*, 33(16).
- Béjar-Pizarro, M., Socquet, A., Armijo, R., Carrizo, D., Genrich, J., and Simons, M. (2013). Andean structural control on interseismic coupling in the North Chile subduction zone. *Nature Geoscience*, 6(6), 462-467.
- Bekaert, D. P., Hooper, A. J., Pathier, E., and Yun, S. (2010). InSAR time series analysis of the 2006 slow slip event on the Guerrero Subduction Zone, Mexico. In *AGU Fall Meeting Abstracts* (Vol. 1, p. 03).
- Bell, J. W., Amelung, F., Ferretti, A., Bianchi, M., and Novali, F. (2008). Permanent scatterer InSAR reveals seasonal and long-term aquifer-system response to groundwater pumping and artificial recharge. *Water Resources Research*, 44(2).
- Berardino, P. G. Fornaro, R. Lanari, E. Sansosti (2002). A new algorithm for surface deformation monitoring based on small baseline differential SAR interferograms. *IEEE Transactions on Geoscience and Remote Sensing*. 40, 2375–2383
- Bhanumurthy, V., Manjusree, P., Srinivasa, Rao, G., (2010). *Flood disaster management*. In remote sensing applications, Roy, P.S., Dwivedi, R.S., Vijayan, D., (eds). National Remote Sensing Centre, India.
- Bhattacharya, A. K. (2013). An analysis of land subsidence in Bangkok and Kolkata due to over-extraction of groundwater. *Electronic Journal of Geotechnical Engineering*, 18, 1683-1694.
- Biggs, J., Bergman, E., Emmerson, B., Funning, G. J., Jackson, J., Parsons, B., and Wright, T. J. (2006). Fault identification for buried strike-slip earthquakes using InSAR: The 1994 and 2004 Al Hoceima, Morocco earthquakes. *Geophysical Journal International*, 166(3). 1347-1362.

- Biggs, J., Wright, T., Lu, Z., and Parsons, B. (2007). Multi-interferogram method for measuring interseismic deformation: Denali Fault, Alaska. *Geophysical Journal International*, 170(3). 1165-1179.
- Bilko, (2010) retrieved 23 June 2014, from [ftp://ftp.noc.soton.ac.uk/mopedftp/extrabilkodata/EnvSchool\\_2010\\_Bilko/EO\\_material/d1\\_SAR\\_land\\_apps\\_lesson/sar\\_land\\_apps\\_1\\_theory.pdf](ftp://ftp.noc.soton.ac.uk/mopedftp/extrabilkodata/EnvSchool_2010_Bilko/EO_material/d1_SAR_land_apps_lesson/sar_land_apps_1_theory.pdf)
- Bo, M. W., and Chu, J. (2006). Impact of geological conditions on ground improvement projects. IAEG2006 The Geological Society of London 2006 Paper number 503
- Bo, M. W., Bawajee, R. and Choa, V. (2001). "Reclamation using dredged materials". Proceedings of the international conference on Port and Maritime R and D and Technology, Singapore, Vol.1, pp.455-461.
- Bock, Y., Wdowinski, S., Ferretti, A., Novali, F., and Fumagalli, A. (2012). Recent subsidence of the Venice Lagoon from continuous GPS and interferometric synthetic aperture radar. *Geochemistry, Geophysics, Geosystems*, 13(3).
- Bonny, M. Tan. (2001) retrieved on 4 August 2014 from [http://eresources.nlb.gov.sg/infopedia/articles/SIP\\_574\\_2004-12-23.html](http://eresources.nlb.gov.sg/infopedia/articles/SIP_574_2004-12-23.html)
- Brigham, C. I. Kolkowitz, M. Dolson, J. Rudy, A. Brooks, C. Hiatt, C. Schmidt, and J. W. Skiles. (2006) *Object-Oriented Analysis of Sea Ice Fragmentation Using SAR Imagery to Determine Pacific Walrus Habitat*. AGU Fall Meeting, Dec. 11-15, San Francisco , CA .
- Bringemeier, D. (2001). *Evaluation of the effects on the groundwater regimes due to groundwater withdrawal at Bukit Tatom, Mukim of Tanjung Dua Belas, Kuala Langat District, Selangor Darul Ehsan*, prepared for Perunding Utama Sdn Bhd, unpublished
- Buckheit, J. B., and D. L. Donoho (1995). *WaveLab and reproducible research*, report, 27 pp., Dep. of Stat., Stanford Univ., Stanford, California
- Budhu, M., and Adiyaman, I. (2013). The influence of clay zones on land subsidence from groundwater pumping. *Groundwater*, 51(1). 51-57.
- Bürgmann, R., Rosen, P. A., and Fielding, E. J. (2000). *Synthetic aperture radar interferometry to measure Earth's surface topography and its deformation*. Annual Review of Earth and Planetary Sciences, 28(1), 169-209.

- Bürgmann, R., D. Schmidt, R. M. Nadeau, M. d'Alessio, E. Fielding, D. Manaker, T. V. McEvelly, and M. H. Murray (2000). Earthquake potential along the northern Hayward fault, California, *Science*, 289, 1178–1182.
- Cai, G., Zhang, A., Zhuo, S., Feng, D., and Sun, M. (2013). An Algorithm of Filtering InSAR Interferogram Based on the Combination of Wavelet Transform and Sigma Filter. *International Conference on Remote Sensing, Environment and Transportation Engineering (RSETE 2013)*. Atlantis Press.
- Calderhead, A. I., Therrien, R., Rivera, A., Martel, R., and Garfias, J. (2011). Simulating pumping-induced regional land subsidence with the use of InSAR and field data in the Toluca Valley, Mexico. *Advances in Water Resources*, 34(1). 83-97.
- Cao, L., Zhang, Y., He, J., Liu, G., Yue, H., Wang, R., and Ge, L. (2008). Coal Mine Land Subsidence Monitoring By Using Spaceborne Insar Data-A Case Study In Fengfeng, Hebei Province, China. *Int. Arch. Photogramm. Remote Sens. Spat. Inf. Sci*, 37, 255-261.
- Capková, I., David, D., and Halounová, L. (2007). Detecting land deformation in the area of northern bohemia using insar stacks (preliminary results). In *Proceedings of* (Vol. 25).
- Capková, I., Kianicka, J., and Halounová, L. (2005). New results of interferometric processing of the northern Bohemia scenes.
- Casu, F. (2009) *The Small Baseline Subset technique: performance assessment and new developments for surface deformation analysis of very extended areas*. Ph.D. in Electronic and Computer Engineering Dept. of Electrical and Electronic Engineering University of Cagliari
- Casu, F., Manzo, M., Lanari, R.A. (2006). Quantitative assessment of the SBAS algorithm performance for surface deformation retrieval from DInSAR data *J. Remote Sens. Environ.*, 102 pp. 195–210
- Catalao, J., Raju, D., and Fernandes, R. M. S. (2013). Mapping Vertical Land Movement In Singapore Using InSAR GPS. In *ESA Special Publication* (Vol. 722, p. 54).
- Cavalié, O., Lasserre, C., Doin, M. P., Peltzer, G., Sun, J., Xu, X., and Shen, Z. K. (2008). Measurement of interseismic strain across the Haiyuan fault (Gansu, China). by InSAR. *Earth and Planetary Science Letters*, 275(3). 246-257.

- Chand, F. (1998). Environmental Geology in Urban Development. *Proc. Geosea*, 98, 329-335.
- Chapin, E., Chan, S. F., Chapman, B. D., Chen, C. W., Martin, J. M., Michel, T. R., and Rosen, P. A. (2006). Impact of the ionosphere on an L-band space based radar. In *Radar, 2006 IEEE Conference on* (pp. 8-pp).
- Chatterjee RS, Lakhera RC, Dadhwal VK (2010) *InSAR coherence and phase information for mapping environmental indicators of opencast coal mining: a case study in Jharia Coalfield, Jharkhand, India*. *Can J Rem Sens* 36:361–373
- Chaussard, E., Amelung, F., Abidin, H., and Hong, S. H. (2013). Sinking cities in Indonesia: ALOS PALSAR detects rapid subsidence due to groundwater and gas extraction. *Remote Sensing of Environment*, 128, 150-161.
- Chaussard, E., Wdowinski, S., Cabral-Cano, E., and Amelung, F. (2014). Land subsidence in central Mexico detected by ALOS InSAR time-series. *Remote Sensing of Environment*, 140, 94-106.
- Chen, A. C., and Zebker, H. A. (2014). Reducing ionospheric effects in InSAR data using accurate coregistration. *IEEE transactions on geoscience and remote sensing*, 52(1). 60-70.
- Chen, C. and Zebker, H. (2000). Network approaches to two-dimensional phase unwrapping: intractability and two new algorithms. *Journal of the Optical Society of America A*, 17: 401–414.
- Chen, C. W., and Zebker, H. A. (2001). Two-dimensional phase unwrapping with use of statistical models for cost functions in nonlinear optimization. *JOSA A*, 18(2), 338-351.
- Chen, C. W., and Zebker, H. A. (2002). Phase unwrapping for large SAR interferograms: statistical segmentation and generalized network models. *Geoscience and Remote Sensing, IEEE Transactions on*, 40(8). 1709-1719.
- Chen, J., and Zebker, H. A. (2012). Ionospheric artifacts in simultaneous L-band InSAR and GPS observations. *Geoscience and Remote Sensing, IEEE Transactions on*, 50(4). 1227-1239.
- Choa, V. (1994). Application of the observational method to hydraulic fill reclamation projects. *Geotechnique*, 44(4). 735-745.

- Colesanti, C., Ferretti, A., Prati, C., and Rocca, F. (2003). Monitoring landslides and tectonic motions with the Permanent Scatterers Technique. *Engineering Geology*, 68(1). 3-14.
- Çomut, F. C., Üstün, A. (2012) *Impact of Perpendicular and Temporal Baseline Characteristics on InSAR Coherence Maps*. TurkeyFIG Working Week: Knowing to manage the territory, protect the environment, evaluate the cultural heritage. Rome, Italy.
- Crosetto, M., Biescas, E., Duro, J., Closa, J., and Arnaud, A. (2008). Generation of advanced ERS and Envisat interferometric SAR products using the stable point network technique. *Photogrammetric Engineering and Remote Sensing*, 74(4), 443-450.
- Dammert, P. B. G., (1996). *Accuracy of INSAR measurements in forested areas*. In Proceedings of ESA Fringe Workshop on ERS SAR Interferometry, Zurich, Switzerland, (Noordwijk, The Netherlands: ESA). SP-406, pp. 37–49.
- Delacourt, C., Briole, P., and Achache, J. A. (1998). Tropospheric corrections of SAR interferograms with strong topography. Application to Etna. *Geophysical Research Letters*, 25(15). 2849-2852.
- D'errico, J. R. (1991). *U.S. Patent No. 4,992,861*. Washington, DC: U.S. Patent and Trademark Office.
- Ding, X. L., Liu, G. X., Li, Z. W., Li, Z. L., and Chen, Y. Q. (2004). Ground subsidence monitoring in Hong Kong with satellite SAR interferometry. *Photogrammetric Engineering and Remote Sensing*, 70(10). 1151-1156.
- Doin, M. P., Lasserre, C., Peltzer, G., Cavalié, O., and Doubre, C. (2009). Corrections of stratified tropospheric delays in SAR interferometry: Validation with global atmospheric models. *Journal of Applied Geophysics*, 69(1). 35-50.
- Dong, S., Samsonov, S., Yin, H., Ye, S., and Cao, Y. (2014). Time-series analysis of subsidence associated with rapid urbanization in Shanghai, China measured with SBAS InSAR method. *Environmental earth sciences*, 72(3), 677-691.
- Earthdef (2016), retrieved on 19 April 2016 from  
<http://earthdef.caltech.edu/attachments/246/20101120.xml>
- Eichel, C., Krämer, M., Schütz, L., and Wurzler, S. (1996). The water-soluble fraction of atmospheric aerosol particles and its influence on cloud

- microphysics. *Journal of Geophysical Research: Atmospheres* (1984–2012).101(D23). 29499-29510.
- Eineder M., Minet C., Steigenberger P., Cong X.,and Fritz T. (2011). Imaging geodesy—toward centimeter-level ranging accuracy with TerraSAR-X. *IEEE Trans. Geosci. Remote Sens.*; 49(2):661-671
- Eineder, M. (2003). Problems and solutions for InSAR digital elevation model generation of mountainous terrain. In *ESA FRINGE workshop, ESA, Frascati*.
- ESA (2013) retrieved on 31 December, 2013 from [http://www.esa.int/Education/Educational\\_material\\_from\\_ESA](http://www.esa.int/Education/Educational_material_from_ESA)
- Fan, H., Deng, K., Ju, C., Zhu, C., and Xue, J. (2011). Land subsidence monitoring by D-InSAR technique. *Mining Science and Technology (China)*.21(6). 869-872.
- Farooque, M.A. and Rohankar, J.S., (2013). Survey on various noises and techniques for denoising the color image. *International Journal of Application or Innovation in Engineering and Management (IJAIEEM)*, 2(11), pp.217-221.
- Fattahi, H., and Amelung, F. (2013). DEM error correction in InSAR time series. *Geoscience and Remote Sensing, IEEE Transactions on*, 51(7). 4249-4259.
- Fattahi, H., and Amelung, F. (2014). InSAR uncertainty due to orbital errors. *Geophysical Journal International*, 199(1). 549-560.
- Feng, G. (2011). *Coseismic deformation and ionospheric variation associated with Wenchuan earthquake estimated from InSAR*. Doctoral dissertation, The Hong Kong Polytechnic University.
- Feng, G., Ding, X., Li, Z., Mi, J., Zhang, L., and Omura, M. (2012). Calibration of an InSAR-derived coseismic deformation map associated with the 2011 Mw-9.0 Tohoku-Oki earthquake. *Geoscience and Remote Sensing Letters, IEEE*, 9(2). 302-306.
- Feng, G., Hetland, E. A., Ding, X., Li, Z., and Zhang, L. (2010). Coseismic fault slip of the 2008 Mw 7.9 Wenchuan earthquake estimated from InSAR and GPS measurements. *Geophysical research letters*, 37(1).
- Ferretti, A., C. Prati, and F. Rocca, (1999). *Monitoring terrain deformation using multi-temporal SAR images*, Proceedings of the CEOS SAR Workshop, 26-29 October, Toulouse, France, (on CD ROM)

- Ferretti, A., Prati, C., and Rocca, F. (1999). Multibaseline InSAR DEM reconstruction: The wavelet approach. *IEEE Transactions on Geoscience and Remote Sensing*, 37(2), 705-715.
- Ferretti, A., Prati, C., and Rocca, F. (2000). Nonlinear subsidence rate estimation using permanent scatterers in differential SAR interferometry. *Geoscience and Remote Sensing, IEEE transactions on*, 38(5). 2202-2212.
- Ferretti, A., Prati, C., and Rocca, F. (2001). Permanent scatterers in SAR interferometry. *Geoscience and Remote Sensing, IEEE Transactions on*, 39(1). 8-20.
- Ferretti, A., Savio, G., Barzaghi, R., Borghi, A., Musazzi, S., Novali, F., and Rocca, F. (2007). Submillimeter accuracy of InSAR time series: Experimental validation. *IEEE Transactions on Geoscience and Remote Sensing*, 45(5), 1142-1153.
- Fialko, Y., Sandwell, D., Simons, M., and Rosen, P. (2005). Three-dimensional deformation caused by the Bam, Iran, earthquake and the origin of shallow slip deficit. *Nature*, 435(7040). 295-299.
- Fraczek, W. (2003). Mean sea level, GPS, and the geoid. *ArcUsers Online*.
- Franceschetti, G., and Lanari, R. (1999). *Synthetic aperture radar processing*. CRC press.
- Frei U., C. Graf, and E. Meier, (1993). *Cartographic reference system, Chapter 10 in SAR-Geocoding - Data and Systems*, WichmannVerlag, edited by Schreier,.
- Frost, V. S., Stiles, J. A., Shanmugan, K. S., and Holtzman, J. (1982). A model for radar images and its application to adaptive digital filtering of multiplicative noise. *Pattern Analysis and Machine Intelligence, IEEE Transactions on*, (2). 157-166.
- Fruneau, B., J.P. Rudant, D. Obert, and D. Raymond, (1999). Small displacements detected by SAR interferometry on the City of Paris (France). Proceedings of IGARSS'99, 28 June-02 July, Hamburg, Germany, (on CD ROM)
- Gabriel, A. K., Goldstein, R. M., and Zebker, H. A. (1989). Mapping small elevation changes over large areas: differential radar interferometry. *Journal of Geophysical Research: Solid Earth (1978–2012)*. 94(B7). 9183-9191.
- Galloway, D. L., D. R. Jones, and S. E. Ingebritsen, (1999). Land subsidence in the United States, *U.S. Geol. Surv. Circ. 1182*.

- Gatelli, F., Guamieri, A. M., Parizzi, F., Pasquali, P., Prati, C., and Rocca, F. (1994). The wavenumber shift in SAR interferometry. *Geoscience and Remote Sensing, IEEE Transactions on*, 32(4). 855-865.
- Ge, L., Chang, H. C., and Rizos, C. (2004). Satellite radar interferometry for mine subsidence monitoring. In 22nd Australian Institute of Mine Surveyors Annual Seminar.
- Ghiglia, D. and Romero, L., (1994). Robust two-dimensional weighted and unweighted phase unwrapping using fast transforms and iterative methods, *J. Opt. Soc. Am. A*, 11, 107–117
- Gili, J. A., Corominas, J., and Rius, J. (2000). Using Global Positioning System techniques in landslide monitoring. *Engineering Geology*, 55(3). 167-192.
- GIM (2016) retrieved on 28 June 2016 from <http://www.gim-international.com/content/article/satellite-radar-interferometry>
- Goldstein, R. M., and C. L. Werner, (1997) Radar Ice Motion Interferometry, Proc. 3 *ERS ESA Symposium*, ESA SP-JiJ, 969-972,
- Goldstein, R. M., and Werner, C. L. (1998). Radar interferogram filtering for geophysical applications. *Geophysical Research Letters*, 25(21). 4035-4038.
- Goldstein, R. M., Engelhardt, H., Kamb, B., and Frolich, R. M. (1993). Satellite radar interferometry for monitoring ice sheet motion: application to an Antarctic ice stream. *Science*, 262(5139). 1525-1530.
- Goldstein, R. M., Zebker, H. A., and Werner, C. L. (1988). Satellite radar interferometry: Two-dimensional phase unwrapping. *Radio science*, 23(4). 713-720.
- Goudarzi, M.A., (2010). Detection and measurement of land deformations caused by seismic events using InSAR, sub-pixel correlation and inversion techniques. Thesis (MSc). University of Twente Faculty of Geo-Information and Earth Observation (ITC). pp 127.
- Gourmelen, N., Amelung, F., and Lanari, R. (2010). Interferometric synthetic aperture radar–GPS integration: Interseismic strain accumulation across the Hunter Mountain fault in the eastern California shear zone. *Journal of Geophysical Research: Solid Earth (1978–2012)*. 115(B9).
- Gourmelen, N., Amelung, F., Casu, F., Manzo, M., and Lanari, R. (2007). Mining-related ground deformation in Crescent Valley, Nevada: Implications for sparse GPS networks. *Geophysical Research Letters*, 34(9).

- Graham, L. C. (1974). Synthetic interferometer radar for topographic mapping. *Proceedings of the IEEE*, 62(6), 763-768.
- Graham, J., and Yin, J. H. (2001). On the time-dependent stress-strain behaviour of soft soils. *Soft Soil Engineering*, 13-23.
- GSI, 2004 retrieved on 2 February, 2014 from <http://vldb.gsi.go.jp/sokuchi/sar/mechanism/mechanism03-e.html>
- Gupta, P., R. Hasan, and U. Kumar. (2009). Big Reforms but Small Payoffs: Explaining the Weak Record of Growth in Indian Manufacturing, S. Bery, B. Bosworth, and A. Panagariya (eds). *India Policy Forum*, volume 5, pp 59-108.
- Hanssen, R. F. (2001). *Radar interferometry: data interpretation and error analysis* (Vol. 2). Springer Science and Business Media.
- Hanssen, R. F., and Klees, R. (1998). Applications of SAR Interferometry In Terrestrial And Atmospheric Mapping. In European Microwave week (pp. 5-9).
- Hauser, J. P. (1989). Effects of deviations from hydrostatic equilibrium on atmospheric corrections to satellite and lunar laser range measurements. *Journal of Geophysical Research: Solid Earth*, 94(B8), 10182-10186.
- Hellwich, O. (1999). Basic principles and current issues of SAR interferometry. In *Joint Workshop of ISPRS WGI/1, I/3 and IV/4, Sensors and Mapping from Space*.
- Herrera, G., Toms, R., Lopez-Sanchez, J.M., Delgado, J., Mallorqui, J.J., Duque, S. and Mulas, J., (2007). Advanced DInSAR analysis on mining area : La Union case study (Murcia, SE Sapin). *Engineering Geology*, 90, 148–159 p.
- Hetland, E. A., Musé, P., Simons, M., Lin, Y. N., Agram, P. S., and DiCaprio, C. J. (2012). Multiscale InSAR time series (MInTS) analysis of surface deformation. *Journal of Geophysical Research: Solid Earth (1978–2012)*.117(B2).
- Hooper, A. (2008). A multi-temporal InSAR method incorporating both persistent scatterer and small baseline approaches. *Geophysical Research Letters*, 35(16).
- Hooper, A., and Zebker, H. A. (2007). Phase unwrapping in three dimensions with application to InSAR time series. *JOSA A*, 24(9), 2737-2747.
- Hooper, A., Zebker, H., Segall, P., and Kampes, B. (2004). A new method for measuring deformation on volcanoes and other natural terrains using InSAR persistent scatterers. *Geophysical research letters*, 31(23).

- Hsu, Y. Y., Gonzalez, M., Bossuyt, F., Axisa, F., Vanfleteren, J., and De Wolf, I. (2010). The effect of pitch on deformation behavior and the stretching-induced failure of a polymer-encapsulated stretchable circuit. *Journal of Micromechanics and Microengineering*, 20(7), 075036.
- Hu, J., Li, Z. W., Ding, X. L., Zhu, J. J., Zhang, L., and Sun, Q. (2014). Resolving three-dimensional surface displacements from InSAR measurements: A review. *Earth-Science Reviews*, 133, 1-17.
- Huby, M. (2001). The sustainable use of resources on a global scale. *Social Policy and Administration*, 35(5). 521-537.
- Idrus, S., Abdul, H. H. S., and Ahmad, F. M., (2004). Analyses of Land Use and Land Cover Changes 1974-2001 In Langat Basin, Malaysia Using Geographical Information System (GIS). *Proceedings Of The 2003 Langat Basin Ecosystem research Symposium*. Penerbit LESTARI, UKM.
- Ikehara, M. E., and Phillips Steven, P. (1994). Determination of Land Subsidence Related to Ground-Water-Level Declines Using GPS and Leveling Surveys in Antelope Valley, California 1992. *US Geological Survey, Water Resources Investigations Report*, 4184.
- Imakiire, T., and Koarai, M. (2012). Wide-area land subsidence caused by “the 2011 Off the Pacific Coast of Tohoku Earthquake”. *Soils and Foundations*, 52(5). 842-855.
- Jehle, M., Small, D., Meier, E., and Nüesch, D. (2004). Improved knowledge of SAR geometry through atmospheric modelling. In *Proc. EUSAR* (Vol. 3).
- Jiang, L., and Lin, H. (2010). Integrated analysis of SAR interferometric and geological data for investigating long-term reclamation settlement of Chek Lap Kok Airport, Hong Kong. *Engineering Geology*, 110(3). 77-92.
- Jolivet, R., Agram, P. S., Lin, N. Y., Simons, M., Doin, M. P., Peltzer, G., and Li, Z. (2014). Improving InSAR geodesy using global atmospheric models. *Journal of Geophysical Research: Solid Earth*, 119(3), 2324-2341.
- Jolivet, R., Grandin, R., Lasserre, C., Doin, M. P., and Peltzer, G. (2011). Systematic InSAR tropospheric phase delay corrections from global meteorological reanalysis data. *Geophysical Research Letters*, 38(17).
- Joughin, I., Tulaczyk, S., Fahnestock, M., and Kwok, R. (1996). A mini-surge on the Ryder Glacier, Greenland, observed by satellite radar interferometry. *Science*, 274(5285). 228-230.

- Joyce, K. E., Belliss, S. E., Samsonov, S. V., McNeill, S. J., and Glassey, P. J. (2009). A review of the status of satellite remote sensing and image processing techniques for mapping natural hazards and disasters. *Progress in Physical Geography*.
- Jung, H. S., Lee, D. T., Lu, Z., and Won, J. S. (2013). Ionospheric correction of SAR interferograms by multiple-aperture interferometry. *Geoscience and Remote Sensing, IEEE Transactions on*, 51(5). 3191-3199.
- Jung, H. S., Won, J. S., and Kim, S. W. (2009). An improvement of the performance of multiple-aperture SAR interferometry (MAI). *Geoscience and Remote Sensing, IEEE Transactions on*, 47(8). 2859-2869.
- Kampes, B. M. (2005). *Displacement parameter estimation using permanent scatterer interferometry*, Doctoral dissertation, TU Delft, Delft University of Technology.
- Kampes, B. M. (2006). *Radar Interferometry*. Springer.
- Kaneko, Y., Y. Fialko, D. T. Sandwell, X. Tong, and M. Furuya (2013). Interseismic deformation and creep along the central section of the North Anatolian fault (Turkey): InSAR observations and implications for rate-and-state friction properties, *J. Geophys. Res. Solid Earth*, 118, 316–331.
- Karunaratne G P, Yong K Y, Tan T S, Tan S A, Liang K. M, Lee S L and Vijiaratnam A. (1990). Layered clay-sand scheme reclamation at Changi South Bay. Proc. 10th Southeast Asian Geotech. Conf, Taipei,1, 71–76.
- Katen, A. T., Kampes, B., and Bree, R. V. (2001). Tianjin InSAR Land Subsidence Observation Demonstration project. *Delft University Delft*.
- Kausika, B. B. (2013). Polarimetric Modeling of Lunar Surface for Scattering Information Retrieval Using Mini-SAR Data of CHANDRAYAAN-1. *M. Sc. dissertation, University of Twente, Enschede, The Netherlands*,, 30.
- Keeratikasikorn, C., and Trisirisatayawong, I. (2011). A Method to Use Modis Water Vapor Products For Correction of Atmospheric-Induced Phase in Interferogram. *Artificial Satellites*, 46(2), 47-62.
- Knospe, S., and Jonsson, S. (2010). Covariance estimation for dInSAR surface deformation measurements in the presence of anisotropic atmospheric noise. *IEEE Transactions on Geoscience and Remote Sensing*, 48(4), 2057-2065.
- Kociolek, M., Materka, A., Strzelecki, M., and Szczypiński, P. (2001). Discrete wavelet transform-derived features for digital image texture analysis.

- In *International Conference on Signals and Electronic Systems, Łódź-Poland* (pp. 99-104).
- Kohlhase, A. O., Feigl, K. L., and Massonnet, D. (2003). Applying differential InSAR to orbital dynamics: a new approach for estimating ERS trajectories. *Journal of Geodesy*, 77(9). 493-502.
- Lanari, R., Casu, F., Manzo, M., Zeni, G., Berardino, P., Manunta, M., and Pepe, A. (2007). An overview of the small baseline subset algorithm: A DInSAR technique for surface deformation analysis. *Pure and Applied Geophysics*, 164(4). 637-661.
- Lanari, R., Fornaro, G., Riccio, D., Migliaccio, M., Papathanassiou, K. P., Moreira, J. R., and Coltelli, M. (1996). Generation of digital elevation models by using SIR-C/X-SAR multifrequency two-pass interferometry: the Etna case study. *Geoscience and Remote Sensing, IEEE Transactions on*, 34(5). 1097-1114.
- Lanari, R., Lundgren, P., Manzo, M., and Casu, F. (2004). Satellite radar interferometry time series analysis of surface deformation for Los Angeles, California. *Geophysical Research Letters*, 31(23).
- Lauknes, T. R. (2010) *Rockslide Mapping in Norway by Means of Interferometric SAR Time Series Analysis*, A dissertation for the degree of Philosophiae Doctor, Faculty Of Science Department Of Physics And Technology, university of Tromsø
- Lauknes, T. R., Dehls, J., Larsen, Y., Høgda, K. A., and Weydahl, D. J. (2006). A comparison of SBAS and PS ERS InSAR for subsidence monitoring in Oslo, Norway. In *Fringe 2005 Workshop* (Vol. 610).
- Leake, S. A. (1997). Land subsidence from ground-water pumping. US Geological Survey.
- Lee C.W., Z. Lu, H.S. Jung, J.S. Won, D. Dzurisin (2010) *Surface deformation of Augustine Volcano (Alaska), 1992–2005, from multiple-interferogram processing using a refined SBAS InSAR approach*. U.S. Geological Survey Professional Paper 1769, pp. 453–465
- Lee J. C and Rho T., (2001) Application to Leveling Using Total Station, New Technology for a New Century International Conference, FIG Working Week 2001, Seoul, Korea 6–11 May 2001 Session 17 - The Use of Positioning and Measurement Technology in Engineering and Construction Applications

- Lee S L, Karunaratne G P, Yong KY, Tan S A, Tan T S and Vijiaratnam A. (1990) Development in land reclamation. Proc. Convention of Instn. Engr., Singapore, 1990:13-20.
- Lee, H. (2001). *Interferometric synthetic aperture radar coherence imagery for land surface change detection* (Doctoral dissertation, Huxley School, Imperial College, London 2001).
- Lee, H. (2016) retrieved on 28 January 2016 from <http://sar.kangwon.ac.kr/>
- Lee, H., and Liu, J. G. (2000). Topographic phase corrected coherence estimation using multi-pass differential SAR interferometry: differential coherence. In *Geoscience and Remote Sensing Symposium, 2000. Proceedings. IGARSS 2000. IEEE 2000 International Vol. 2*, pp. 776-778.
- Lee, Y. L., Kim, H. C., and Park, H. W. (1998). Blocking effect reduction of JPEG images by signal adaptive filtering. *Image Processing, IEEE Transactions on*, 7(2). 229-234.
- Leung C F, Wong J C, Manivanann R and Tan S A. (2001). Experimental evaluation of consolidation behaviour of stiff clay lumps in reclamation fill. *Geotech. Testing J.* 2001, 24(2): 145-156.
- Li, F. K., and Goldstein, R. M. (1990). Studies of multibaseline spaceborne interferometric synthetic aperture radars. *Geoscience and Remote Sensing, IEEE Transactions on*, 28(1). 88-97.
- Li, T., Liu, G., Jia, H., Lin, H., Zhang, R., Yu, B., and Luo, Q. (2013). *An Improved Multi-Temporal InSAR Method for Increasing Spatial Resolution of Surface Deformation Measurements*. ISPRS-International Archives of the Photogrammetry, Remote Sensing and Spatial Information Sciences, 1(2), 145-150.
- Li, Z. (2004). Production of regional 1 km  $\times$  1 km water vapor fields through the integration of GPS and MODIS data, *ION GNSS 2004*, 21 – 24 Sept, Inst. of Navig., Long Beach, California.
- Li, Z. W., Ding, X. L., Huang, C., Zhu, J. J., and Chen, Y. L. (2008). Improved filtering parameter determination for the Goldstein radar interferogram filter. *ISPRS Journal of Photogrammetry and Remote Sensing*, 63(6). 621-634.
- Li, Z., and Bethel, J. (2008). Image coregistration in SAR interferometry. *Proc. Int. Arch. Photogramm., Remote Sens. Spatial Inf. Sci.*, 433-438.

- Lin, Y. N. N., Simons, M., Hetland, E. A., Muse, P., and DiCaprio, C. (2010). A multiscale approach to estimating topographically correlated propagation delays in radar interferograms. *Geochemistry, Geophysics, Geosystems*, 11(9).
- Lin, Z., Huili, G., Xiaojuan, L., Yaoming, S., and Lingling, J. (2009). Research on driving factors of land subsidence with remote sensing technology. In *Geoscience and Remote Sensing Symposium, 2009 IEEE International, IGARSS 2009* (Vol. 2, pp. II-396).
- Liu, G., Buckley, S. M., Ding, X., Chen, Q., and Luo, X. (2009). Estimating spatiotemporal ground deformation with improved permanent-scatterer radar interferometry. *Geoscience and Remote Sensing, IEEE Transactions on*, 47(8). 2762-2772
- Liu, G., Ding, X., Chen, Y., Li, Z., and Li, Z. (2001). Ground settlement of Chek Lap Kok Airport, Hong Kong, detected by satellite synthetic aperture radar interferometry. *Chinese Science Bulletin*, 46(21). 1778-1782.
- Liu, G., Luo, X., Chen, Q., Huang, D., and Ding, X. (2008). Detecting land subsidence in Shanghai by PS-networking SAR interferometry. *Sensors*, 8(8). 4725-4741.
- Liu, P. (2012). *InSAR observations and modeling of Earth surface displacements in the Yellow River Delta (China)* Doctoral dissertation, University of Glasgow.
- Liu, Z., Jung, H. S., and Lu, Z. (2014). Joint correction of ionosphere noise and orbital error in L-band SAR interferometry of interseismic deformation in southern California. *Geoscience and Remote Sensing, IEEE Transactions on*, 52(6). 3421-3427.
- Löfgren, J. S., Björndahl, F., Moore, A. W., Webb, F. H., Fielding, E. J., and Fishbein, E. F. (2010). Tropospheric correction for InSAR using interpolated ECMWF data and GPS Zenith Total Delay from the Southern California integrated GPS network. In *Geoscience and Remote Sensing Symposium (IGARSS), 2010 IEEE International* (pp. 4503-4506).
- López-Quiroz, P., Doin, M. P., Tupin, F., Briole, P., and Nicolas, J. M. (2009). Time series analysis of Mexico City subsidence constrained by radar interferometry. *Journal of Applied Geophysics*, 69(1). 1-15.
- Lu, Z., and Dzurisin, D. (2014). InSAR Imaging of Aleutian Volcanoes. In *InSAR Imaging of Aleutian Volcanoes* (pp. 87-345). Springer Berlin Heidelberg.

- Lu, Z., Patrick, M., Fielding, E. J., and Trautwein, C. (2003). Lava volume from the 1997 eruption of Okmok volcano, Alaska, estimated from spaceborne and airborne interferometric synthetic aperture radar. *IEEE Trans. Geosci. Remote Sens.*, 41(6). 1428-1436.
- Lundgren, P., Hetland, E. A., Liu, Z., and Fielding, E. J. (2009). Southern San Andreas-San Jacinto fault system slip rates estimated from earthquake cycle models constrained by GPS and interferometric synthetic aperture radar observations. *Journal of Geophysical Research: Solid Earth*, 114(B2).
- Luo, Q., Perissin, D., Lin, H., Zhang, Y., and Wang, W. (2014). Subsidence monitoring of Tianjin suburbs by TerraSAR-X persistent scatterers interferometry. *IEEE Journal of Selected Topics in Applied Earth Observations and Remote Sensing*, 7(5), 1642-1650.
- Luzi, G. (2010). *Ground based SAR interferometry: a novel tool for Geoscience*. INTECH Open Access Publisher.
- Mallat, S. (2008). *A Wavelet Tour of Signal Processing: The Sparse Way* (3<sup>rd</sup> ed.) Academic, Burlington, Mass.
- Manzo, M., Berardino, P., Bonano, M., Casu, F., Manunta, M., Pepe, A., and Lanari, R. (2012). A quantitative assessment of DInSAR time series accuracy in volcanic areas: from the first to second generation SAR sensors. In *Geoscience and Remote Sensing Symposium (IGARSS). 2012 IEEE International*. pp. 911-914.
- Massonnet, D. (2008). Parachute satellites for earth observation. *Acta Astronautica*, 63(1). 411-415.
- Massonnet, D., and Feigl, K. L. (1995). Discrimination of geophysical phenomena in satellite radar interferograms. *Geophysical research letters*, 22(12). 1537-1540.
- Massonnet, D., and Feigl, K. L. (1998). Radar interferometry and its application to changes in the Earth's surface. *Reviews of geophysics*, 36(4). 441-500.
- Massonnet, D., Briole, P., and Arnaud, A. (1995). Deflation of Mount Etna monitored by spaceborne radar interferometry.
- Massonnet, D., Rossi, M., Carmona, C., Adragna, F., Peltzer, G., Feigl, K., and Rabaute, T. (1993). The displacement field of the Landers earthquake mapped by radar interferometry. *Nature*, 364(6433). 138-142.
- Meteoblue (2006) retrieved on 28 August 2014 from <https://content.meteoblue.com/en/meteoscool/the-earth/atmosphere>

- Meyer, F., Bamler, R., Jakowski, N., and Fritz, T. (2006). The potential of low-frequency SAR systems for mapping ionospheric TEC distributions. *Geoscience and Remote Sensing Letters, IEEE*, 3(4). 560-564.
- Mohr, J. J., Reeh, N., and Madsen, S. N. (1998). Three-dimensional glacial flow and surface elevation measured with radar interferometry. *Nature*, 391(6664). 273-276.
- Mora, O., Mallorqui, J. J., and Broquetas, A. (2003). Linear and nonlinear terrain deformation maps from a reduced set of interferometric SAR images. *Geoscience and Remote Sensing, IEEE Transactions on*, 41(10). 2243-2253.
- Moreau, F., Dauteuil, O., Bour, O., and Gavrilenko, P. (2006). GPS measurements of ground deformation induced by water level variations into a granitic aquifer (French Brittany). *Terra Nova*, 18(1), 50-54.
- Motagh, M., Djamour, Y., Walter, T. R., Wetzel, H. U., Zschau, J., and Arabi, S. (2007). Land subsidence in Mashhad Valley, northeast Iran: results from InSAR, levelling and GPS. *Geophysical Journal International*, 168(2). 518-526.
- Muço, B., Alexiev, G., Aliaj, S., Elezi, Z., Grecu, B., Mandrescu, N., Milutinovic, Z., Radulian, M., Rangelov, B. and Shkupi, D., (2012). Geohazards assessment and mapping of some Balkan countries. *Natural hazards*, 64(2), pp.943-981.
- MyMetro (2014) retrieved on 23 May 2014 from  
<http://www.hmetro.com.my/node/66640>
- NAP, 2007). retrieved on 2 February, 2014 from  
<https://books.google.com/books?isbn=0309104092>
- NEST (2007) Retrieved on 31 December 2013 from  
<https://earth.esa.int/web/nest/release-notes>
- Nichols, Jr. T.C. Rebound, its nature and effect on engineering works. 1980. *Quarterly Journal of Engineering Geology*. 13133-152.
- Odiijk, D., Kenselaar, F., and Hanssen, R. (2003). Integration of leveling and InSAR data for land subsidence monitoring. In *11th FIG International Symposium on Deformation Measurements*, Santorini, Greece , pp. 23-28.
- Ortega-Guerrero, A., Rudolph, D. L., and Cherry, J. A. (1999). Analysis of long-term land subsidence near Mexico City: Field investigations and predictive modeling. *Water Resources Research*, 35(11), 3327-3341.

- Osmanoğlu, B., Dixon, T. H., Wdowinski, S., Cabral-Cano, E., and Jiang, Y. (2011). Mexico City subsidence observed with persistent scatterer InSAR. *International Journal of Applied Earth Observation and Geoinformation*, 13(1), 1-12.
- Parbleu, 2007 retrieved on 2 February, 2014 from <http://www.parbleu.biz/remsens.htm>
- Park, Y. (1997). Application of a fuzzy linguistic approach to analyse Asian airports' competitiveness. *Transportation Planning and Technology*, 20(4). 291-309.
- Parviz, 2012 retrieved on 2 February, 2014 from <https://parviztarikhi.wordpress.com/features-2/insar-for-aquatic-bodies/>
- Patidar, P., Gupta, M., Srivastava, S. and Nagawat, A.K., (2010). Image de-noising by various filters for different noise. *International Journal of Computer Applications (0975–8887) Volume*.
- Paul Rosen, JPL Eric Fielding, JPL Piyush S. Agram, JPL Matt Pritchard, Cornell Scott Baker, (2014). UNAVCO, INSAR: An Introduction to Processing and Applications for Geoscientists Short Course Unavco, Headquarters - Boulder, Co August 4–6,
- Paylor, A., (1994). *Airport Developments in Asia*. Chichester United Kingdom. MDIS Publications Ltd.
- Pradhan, B., Abokharima, M. H., Jebur, M. N., and Tehrany, M. S. (2014). Land subsidence susceptibility mapping at Kinta Valley (Malaysia) using the evidential belief function model in GIS. *Natural hazards*, 73(2). 1019-1042.
- Prati, C, and Fabio R. (1994). *U.S. Patent No. 5,332,999*. Process for generating synthetic aperture radar interferograms.
- Puysségur, B., Michel, R., and Avouac, J. P. (2007). Tropospheric phase delay in interferometric synthetic aperture radar estimated from meteorological model and multispectral imagery. *Journal of Geophysical Research: Solid Earth (1978–2012)*. 112(B5).
- Qing, X., Guowang, J., Caiying, Z., Zhengde, W., Yu, H., and Peizhang, Y. (2004). The Filtering and Phase Unwrapping of Interferogram. Proc. ISPRS XXXV Comm V1/WG4.
- Rao, Y. S., Deo, R., Nalini, J., Pillai, A. M., Muralikrishnan, S., and Dadhwal, V. K. (2014). Quality assessment of TanDEM-X DEMs using airborne LiDAR, photogrammetry and ICESat elevation data. *ISPRS Annals of the Photogrammetry, Remote Sensing and Spatial Information Sciences*, 2(8), 187.

- Raspini, F., Moretti, S., and Casagli, N. (2013). Landslide mapping using SqueeSAR data: Giampilieri (Italy) case study. In *Landslide science and practice* (pp. 147-154). Springer Berlin Heidelberg.
- Raucoules, D., Colesanti, C., and Carnec, C. (2007). Use of SAR interferometry for detecting and assessing ground subsidence. *Comptes Rendus Geoscience*, 339(5). 289-302.
- Remy, D., Bonvalot, S., Briole, P., and Murakami, M. (2003). Accurate measurements of tropospheric effects in volcanic areas from SAR interferometry data: Application to Sakurajima volcano (Japan). *Earth and Planetary Science Letters*, 213(3). 299-310.
- Rocca *et al.*, (2014) retrieved on 3 April 2016 from <http://earth.esa.int/workshops/ers97/program-details/speeches/rocca-et-al/>
- Rocca, F. (2003). 3D motion recovery with multi-angle and/or left right interferometry, Politecnico di Milano, in Proceedings of the Fringe03 International Meeting ESA, Frascati, Italy, December 2003.
- Rodriguez, E., and Martin, J. M. (1992). Theory and design of interferometric synthetic aperture radars. In *Radar and Signal Processing, IEE Proceedings*. Vol. 139, No. 2, pp. 147-159.
- Rogers, J. D., Olshansky, R., and Rogers, R. B. (1993). Damage to foundations from expansive soils. *Claims People*, 3(4), 1-4
- Rosen, P., E. Gurrola, G. Sacco, and H. A. Zebker (2011). InSAR scientific computing environment— The home stretch, poster IN43B-1397 presented at 2010 Fall Meeting, AGU, San Francisco, Calif., 13–17 Dec
- Rosen, P. A., Hensley, S., Joughin, I. R., Li, F. K., Madsen, S. N., Rodriguez, E., and Goldstein, R. M. (2000). Synthetic aperture radar interferometry. *Proceedings of the IEEE*, 88(3). 333-382.
- Rudenko S., Otten M., Visser P., Scharroo R., Schone T., Esselborn S. (2012) New improved orbit solutions for the ERS-1 and ERS-2 satellites. *Adv. Space Res.* (49),1229-1244.
- Ruescas, A. B., Delgado, J. M., Costantini, F., and Sarti, F. (2009). Change detection by interferometric coherence in Nasca Lines, Peru (1997–2004). *Fringe 2009*, 30.

- Sahu, P., and Sikdar, P. K. (2011). Threat of land subsidence in and around Kolkata City and East Kolkata Wetlands, West Bengal, India. *Journal of earth system science*, 120(3). 435-446.
- Samsonov, S., Tiampo, K., González, P. J., Manville, V., and Jolly, G. (2010). Ground deformation occurring in the city of Auckland, New Zealand, and observed by Envisat interferometric synthetic aperture radar during 2003–2007. *Journal of Geophysical Research: Solid Earth (1978–2012)*. 115(B8).
- Sandwell, D. T., and Price, E. J. (1998). Phase gradient approach to stacking interferograms. *Journal of Geophysical Research: Solid Earth (1978–2012)*. 103(B12). 30183-30204.
- Sandwell, D. T., Myer, D., Mellors, R., Shimada, M., Brooks, B., and Foster, J. (2008). Accuracy and resolution of ALOS interferometry: Vector deformation maps of the Father's Day intrusion at Kilauea. *IEEE Transactions on Geoscience and Remote Sensing*, 46(11), 3524-3534.
- Sarmap (2007) retrieved on 28 January 2015 from [http://www.fgg.uni-lj.si/~alise/WG5/wg5\\_documents/CostaRica2007\\_material/03\\_Generation\\_of\\_Digital\\_Elevation\\_Model\(Costa-Rica2007\).pdf](http://www.fgg.uni-lj.si/~alise/WG5/wg5_documents/CostaRica2007_material/03_Generation_of_Digital_Elevation_Model(Costa-Rica2007).pdf)
- Sarmap (2009) retrieved on 13 March 2015 from <http://www.sarmap.ch/pdf/SAR-Guidebook.pdf>
- Sarti, F., Briole, P., and Pirri, M. (2006). Coseismic fault rupture detection and slip measurement by ASAR precise correlation using coherence maximization: application to a north-south blind fault in the vicinity of Bam (Iran). *Geoscience and Remote Sensing Letters, IEEE*, 3(2). 187-191.
- Scharroo, R., and Visser, P. (1998). Precise orbit determination and gravity field improvement for the ERS satellites. *Journal of Geophysical Research: Oceans*, 103(C4), 8113-8127.
- Schmidt, D. A., and Bürgmann, R. (2003). Time-dependent land uplift and subsidence in the Santa Clara valley, California, from a large interferometric synthetic aperture radar data set. *Journal of Geophysical Research: Solid Earth (1978–2012)*. 108(B9).
- Schwabisch, M. (1998). A fast and efficient technique for SAR interferogram geocoding. In *Geoscience and Remote Sensing Symposium Proceedings, 1998. IGARSS'98. 1998 IEEE International (Vol. 2, pp. 1100-1102)*.

- Schwabisch, M., and Geudtner, D. (1995). Improvement of phase and coherence map quality using azimuth prefiltering: Examples from ERS-1 and X-SAR. In *Geoscience and Remote Sensing Symposium, 1995. IGARSS'95. 'Quantitative Remote Sensing for Science and Applications', International* (Vol. 1, pp. 205-207).
- Schwäbisch, M., Mercer, B., Zhang, Q., and Huang, W. (2010). Accurate focusing of single-pass airborne InSAR data at L-band. In *IGARSS* (pp. 2625-2628).
- Scivier, M. S., Fiddy, M. A., and Burge, R. E. (1986). Estimating SAR phase from complex SAR imagery. *Journal of Physics D: Applied Physics*, 19(3). 357-362
- Sefercik, U. G., and Dana, I. (2011). Crucial points of interferometric processing for dem generation using high resolution sar data. *Polarization*, 15(10), 38-504.
- Shankar, A. K. (2013) *Atmospheric correction of DInSAR phase for land subsidence measurements using an integrated approach* Master, University of Twente, Enschede, The Netherlands
- Shi, X., and Zhang, Y. (2011). Improving Goldstein filter by image entropy for InSAR interferogram filtering. In *Synthetic Aperture Radar (AP SAR). 2011 3rd International Asia-Pacific Conference on* (pp. 1-4).
- Shirzaei, M., and Bürgmann, R. (2012). Topography correlated atmospheric delay correction in radar interferometry using wavelet transforms. *Geophysical Research Letters*, 39(1).
- Shirzaei, M., and Walter, T. R. (2011). Estimating the effect of satellite orbital error using wavelet-based robust regression applied to InSAR deformation data. *Geoscience and Remote Sensing, IEEE Transactions on*, 49(11). 4600-4605.
- Short, N., LeBlanc, A. M., Sladen, W., Oldenborger, G., Mathon-Dufour, V., and Brisco, B. (2014). RADARSAT-2 D-InSAR for ground displacement in permafrost terrain, validation from Iqaluit Airport, Baffin Island, Canada. *Remote Sensing of Environment*, 141, 40-51.
- Simons, M., and Rosen, P. A. (2007). Interferometric synthetic aperture radar geodesy.
- Singh, P. and Arora, A., (2013). Analytical Analysis of Image Filtering Techniques. *International Journal of Engineering and Innovative Technology (IJEIT) Volume*, (4).

- Smolíková J, Blahůt J, Tábořík P, Žížala D, Vilímek V (2013) *Shallow slope deformations triggered by extreme rainfall case studies from the Czech Republic*. In: Proceedings of the 8th IAG International Conference on Geomorphology, Paris, France: 653
- Solari, L., Ciampalini, A., Raspini, F., Bianchini, S., and Moretti, S. (2016). PSInSAR analysis in the Pisa Urban Area (Italy): A case study of subsidence related to stratigraphical factors and urbanization. *Remote Sensing*, 8(2), 120.
- Soni, N. K. (2012). *Phase unwrapping algorithm using edge detection and statistical cost functions* (Doctoral dissertation, TU Delft, Delft University of Technology).
- Sousa, J. J., Hooper, A. J., Hanssen, R. F., Bastos, L. C., and Ruiz, A. M. (2011). Persistent scatterer InSAR: a comparison of methodologies based on a model of temporal deformation vs. spatial correlation selection criteria. *Remote Sensing of Environment*, 115(10), 2652-2663.
- Sowter, A., Bateson, L., Strange, P., Ambrose, K., and Syafiudin, M. F. (2013). DInSAR estimation of land motion using intermittent coherence with application to the South Derbyshire and Leicestershire coalfields. *Remote Sensing Letters*, 4(10), 979-987.
- Stevens, D. R., Cumming, I. G., and Gray, A. L. (1995). Options for airborne interferometric SAR motion compensation. *IEEE Transactions on Geoscience and Remote Sensing*, 33(2), 409-420.
- Strozzi, T., and Wegmuller, U. (1999). Land subsidence in Mexico City mapped by ERS differential SAR interferometry. In *Geoscience and Remote Sensing Symposium, 1999. IGARSS'99 Proceedings. IEEE 1999 International* (Vol. 4, pp. 1940-1942).
- Strozzi, T., G. Bitelli, and U. Wegmiiller, (2000). Differential SAR interferometry for land subsidence mapping in Bologna, Proceedings of SISOLS 2000, 25-29 September, Ravenna, Italy, 2:187-192
- Strozzi, T., Wegmuller, U., Tosi, L., Bitelli, G., and Spreckels, V. (2001). Land subsidence monitoring with differential SAR interferometry. *Photogrammetric engineering and remote sensing*, 67(11). 1261-1270.
- Sudha, S., Suresh, G.R. and Sukanesh, R., (2009). Speckle noise reduction in ultrasound images by wavelet thresholding based on weighted variance. *International journal of computer theory and engineering*, 1(1), p.7.

- Syvitski, J. P., Kettner, A. J., Overeem, I., Hutton, E. W., Hannon, M. T., Brakenridge, G. R., and Nicholls, R. J. (2009). Sinking deltas due to human activities. *Nature Geoscience*, 2(10), 681-686.
- Tarayre, H., and Massonnet, D. (1994). Effects of a refractive atmosphere on interferometric processing. In *Geoscience and Remote Sensing Symposium, 1994. IGARSS'94. Surface and Atmospheric Remote Sensing: Technologies, Data Analysis and Interpretation., International* (Vol. 2, pp. 717-719).
- Tizzani, P., Berardino, P., Casu, F., Euillades, P., Manzo, M., Ricciardi, G. P., and Lanari, R. (2007). Surface deformation of Long Valley caldera and Mono Basin, California, investigated with the SBAS-InSAR approach. *Remote Sensing of Environment*, 108(3). 277-289.
- Tong, X., D. T. Sandwell, and B. Smith-Konter (2013). High-resolution interseismic velocity data along the San Andreas Fault from GPS and InSAR, *J. Geophys. Res. Solid Earth*, 118, 369–389.
- Tourism Malaysia (2007), retrieved on 20 May 2016 from <http://www.tourism.gov.my/media/view/visit-malaysia-year-2007>
- Touzi, R., Lopes, A., Bruniquel, J., and Vachon, P. W. (1999). Coherence estimation for SAR imagery. *Geoscience and Remote Sensing, IEEE Transactions on*, 37(1). 135-149.
- Unavco, (2008) retrieved on 31 January, 2014 from [https://www.unavco.org/education/advancing-geodetic-skills/short-courses/course-materials/insar/2008-insar-course-materials/sar\\_summary.pdf](https://www.unavco.org/education/advancing-geodetic-skills/short-courses/course-materials/insar/2008-insar-course-materials/sar_summary.pdf)
- URETEK, (2014) retrieved on 4 June 2016 from <http://www.uretekworldwide.com/references/infrastructure/re-levelling-international-airport>
- Usai, S. (2003). A least-squares database approach for SAR interferometric data *IEEE Transactions on Geoscience and Remote Sensing*, 41 (4) pp. 753–760
- Utexas (2016) retrieved on 4 January, 2016 from <https://www.lib.utexas.edu/maps/singapore.html>
- Van der Kooij, M., Hughes, W., Sato, S., and Poncos, V. (2005). Coherent target monitoring at high spatial density: examples of validation results. In *Fringe Workshop, European Space Agency*.
- Wadge, G., Webley, P. W., James, I. N., Bingley, R., Dodson, A., Waugh, S., and Clarke, P. J. (2002). Atmospheric models, GPS and InSAR measurements of the

- tropospheric water vapour field over Mount Etna. *Geophysical Research Letters*, 29(19). 11-1.
- Wan, Q., Liew, S. C., and Kwoh, L. K. (2014). Persistent scatterer InSAR for ground deformation mapping using ALOS PALSAR data: A case study in Singapore. In *2014 IEEE Geoscience and Remote Sensing Symposium* (pp. 441-444).
- Wang, H., Wright, T. J., and Biggs, J. (2009). Interseismic slip rate of the northwestern Xianshuihe fault from InSAR data. *Geophysical Research Letters*, 36(3).
- Wang, H., Wright, T. J., Yu, Y., Lin, H., Jiang, L., Li, C., and Qiu, G. (2012). InSAR reveals coastal subsidence in the Pearl River Delta, China. *Geophysical Journal International*, 191(3). 1119-1128.
- Wang, M., Li, T., and Jiang, L. (2016). Monitoring reclaimed lands subsidence in Hong Kong with InSAR technique by persistent and distributed scatterers. *Natural Hazards*, 82(1), 531-543.
- Wegmueller, M. S., Oberle, M., Felber, N., Kuster, N., and Fichtner, W. (2010). Signal transmission by galvanic coupling through the human body. *Instrumentation and Measurement, IEEE Transactions on*, 59(4). 963-969.
- Wegmuller, U., Werner, C., Strozzi, T., and Wiesmann, A. (2006). Ionospheric electron concentration effects on SAR and INSAR. In *Geoscience and Remote Sensing Symposium, 2006. IGARSS 2006. IEEE International Conference on* (pp. 3731-3734). IEEE.
- Wei, M., Sandwell, D., and Smith-Konter, B. (2010). Optimal combination of InSAR and GPS for measuring interseismic crustal deformation. *Advances in Space Research*, 46(2). 236-249.
- Werner, C., Wegmuller U., Strozzi T., and Wiesmann A. (2003). Interferometric point target analysis for deformation mapping, *Proc. Int. Geosci. Remote Sens. Symp.*
- Wikipedia (2016), retrieved on 4 March 2016 from  
[https://en.wikipedia.org/wiki/Tropical\\_climate](https://en.wikipedia.org/wiki/Tropical_climate)
- Wolff, C. (2011) retrieved on 19 September 2015 from  
<http://www.radartutorial.eu/01.basics/Radar%20Principle.en.html>
- Woodhouse, I. H. (2005). *Introduction to microwave remote sensing*. CRC press.

- World Tourism Organization (2012), retrieved on 4 May 2016 from <http://www.thestar.com.my/news/nation/2012/02/17/msia-is-ninth-most-visited-in-the-world-in-unwto-list/>
- Wortham, C. B. (2014). *Vector Deformation Time-series from Spaceborne Motion Compensation InSAR Processors* Doctoral dissertation, Stanford University.
- Wright, T. J., Parsons, B., England, P. C., and Fielding, E. J. (2004). InSAR observations of low slip rates on the major faults of western Tibet. *Science*, 305(5681). 236-239.
- Wu, N., Feng, D. Z., and Li, J. (2006). A locally adaptive filter of interferometric phase images. *Geoscience and Remote Sensing Letters, IEEE*, 3(1). 73-77.
- Xu, H., Dvorkin, J., and Nur, A. (2001). Linking oil production to surface subsidence from satellite radar interferometry. *Geophysical research letters*, 28(7). 1307-1310.
- Yan, Y., Doin, M. P., Lopez-Quiroz, P., Tupin, F., Fruneau, B., Pinel, V., and Trouvé, E. (2012). Mexico city subsidence measured by InSAR time series: Joint analysis using PS and SBAS approaches. *IEEE Journal of Selected Topics in Applied Earth Observations and Remote Sensing*, 5(4), 1312-1326.
- Yan, Y., Lopez-Quiroz, P., Doin, M., Tupin, F., Fruneau, B., (2009). Comparison of two methods in multi-temporal differential SAR interferometry: application to the measurement of Mexico City subsidence. In: *Fringe 2009*, p. 8.
- Yanjie, Z. (2005). A new interferogram generation method. In *Geoscience and Remote Sensing Symposium, 2005. IGARSS'05. Proceedings. 2005 IEEE International* (Vol. 7, pp. 4557-4559).
- Yanjie, Z., and Prinet, V. (2004). InSAR coherence estimation. In *IGARSS* (pp. 3353-3355).
- Yoon, Y. T., Eineder, M., Yague-Martinez, N., and Montenbruck, O. (2009). TerraSAR-X precise trajectory estimation and quality assessment. *Geoscience and Remote Sensing, IEEE Transactions on*, 47(6). 1859-1868.
- Yue, H., Guo, H., Chen, Q., Hanssen, R., Leijen, F., Marinkovic, P., and Ketelaar, G. (2005). Land subsidence monitoring in city area by time series interferometric SAR data. In *International Geoscience And Remote Sensing Symposium* (Vol. 7, p. 4590).
- Zebker, H. A., and Villasenor, J. (1992). Decorrelation in interferometric radar echoes. *Geoscience and Remote Sensing, IEEE Transactions on*, 30(5). 950-959.

- Zebker, H. A., Madsen, S. N., Martin, J., Wheeler, K. B., Miller, T., Lou, Y., and Cucci, A. (1992). The TOPSAR interferometric radar topographic mapping instrument. *Geoscience and Remote Sensing, IEEE Transactions on*, 30(5). 933-940.
- Zebker, H. A., Rosen, P. A., and Hensley, S. (1997). Atmospheric effects in interferometric synthetic aperture radar surface deformation and topographic maps. *Journal of Geophysical Research: Solid Earth (1978–2012)*. 102(B4). 7547-7563.
- Zebker, H. A., Rosen, P. A., Goldstein, R. M., Gabriel, A., and Werner, C. L. (1994). On the derivation of coseismic displacement fields using differential radar interferometry: The Landers earthquake. *Journal of Geophysical Research: Solid Earth (1978–2012)*. 99(B10). 19617-19634.
- Zhang, L., Ding, X., Lu, Z., Jung, H. S., Hu, J., and Feng, G. (2014). A novel multitemporal InSAR model for joint estimation of deformation rates and orbital errors. *Geoscience and Remote Sensing, IEEE Transactions on*, 52(6). 3529-3540.
- Zhang, L., Wu, J. C., Ge, L. L., Ding, X. L., and Chen, Y. L. (2008). Determining fault slip distribution of the Chi-Chi Taiwan earthquake with GPS and InSAR data using triangular dislocation elements. *Journal of Geodynamics*, 45(4). 163-168.
- Zhao, C., Lu, Z., Zhang, Q., and de La Fuente, J. (2012). Large-area landslide detection and monitoring with ALOS/PALSAR imagery data over Northern California and Southern Oregon, USA. *Remote Sensing of Environment*, 124, 348-359.
- Zhao, D., Z. Huang, N. Umino, A. Hasegawa, and H. Kanamori (2011). Structural heterogeneity in the megathrust zone and mechanism of the 2011 Tohoku-oki earthquake (Mw 9.0). *Geophys. Res. Lett.*, 38, L17308.
- Zhao, Q., Lin, H., Chen, F., and Gao, W. (2011). InSAR detection of residual settlement of ocean reclamation areas in Shenzhen, China. In *Geoinformatics, 2011 19th International Conference on* (pp. 1-5).
- Zhao, Q., Lin, H., Gao, W., Zebker, H. A., Chen, A., and Yeung, K. (2011). InSAR detection of residual settlement of an ocean reclamation engineering project: a case study of Hong Kong International Airport. *Journal of oceanography*, 67(4). 415-426.

- Zhou, N. Q., and Zhao, S. (2013). Urbanization process and induced environmental geological hazards in China. *Natural hazards*, 67(2), 797-810.
- Zhou, W., Chen, F., and Guo, H. (2015). Differential radar interferometry for structural and ground deformation monitoring: A new tool for the conservation and sustainability of cultural heritage sites. *Sustainability*, 7(2), 1712-1729.
- Zhou, X., Chang, N. B., and Li, S. (2009). Applications of SAR interferometry in earth and environmental science research. *Sensors*, 9(3), 1876-1912.
- Zhu, G.F., Yin, J.H., and Graham, J. (2001). Consolidation modelling of soils under the Test Embankment at Chek Lap Kok International Airport in Hong Kong using a simplified finite element method. *Canadian Geotechnical Journal*, Vol.38, No.2, 349-363. (SCI 30)
- Zizzi, S. (2013) Real estate disclosure reporting method.U.S. Patent Application 14/104,682.
- Zou, W., Li, Y., Li, Z., and Ding, X. (2009). Improvement of the Accuracy of InSAR Image Co-Registration Based On Tie Points—A Review. *Sensors*, 9(2), 1259-1281.